Spatio-temporal analysis of oak decline process in open woodlands: A case study in SW Spain.

Jesús Fernández-Habas[1], Pilar Fernández-Rebollo[1], Mónica Rivas Casado[2], Alma María García Moreno[1], Begoña Abellanas[1*].

[1]Universidad de Córdoba, Departamento de Ingeniería Forestal, Campus de Rabanales, E-14014 Córdoba, Spain.

[2]Department of Environmental Science and Technology, Cranfield University, Cranfield MK43 0AL, UK

*Corresponding author:

E-mail address: ir1aboab@uco.es (B. Abellanas).

Abstract

This study aims to characterize at landscape level the spatio-temporal dynamics of a massive oak decline that is occurring in *dehesas* ecosystems. We are looking at possibilities of matching with *Phytophthora* disease behavior, a harmful disease detected in the studied area, in order to interpret its implications within the context of the disease management. Spatial locations of affected trees from 2001, 2009 and 2016 identified through photointerpretation were analyzed with the inhomogeneous Ripley's K-function to assess their spatial pattern. Multivariate Adaptive Regression Splines (MARS), a non-parametric data mining method, was used to investigate the influence of a range of landscape descriptors of different nature on the proneness to oak decline, using the location of affected trees in comparison with that of healthy spots (points randomly extracted from areas covered by healthy trees).

Affected trees showed a strong clustering pattern that decreased over time. The reported spatial patterns align with the hypothesis of *Phytophthora cinnamomi* Rands. being the main cause of oak decline in Mediterranean forests. Location of affected trees detected in different years was found to be spatially related, suggesting the implication of a contagion process. MARS models from 2001, 2009 and 2016reported Area Under the Curve (AUC) values of 0.707, 0.671and 0.651,respectively. Slope was the most influential landscape descriptor across the three years, with distance to afforestations being the second for 2001 and 2009. Landscape descriptors linked to human factors and soil water content seem to influence oak decline caused by *Phytophthora cinnamomi* at landscape level. Afforestations carried out as

part of the afforestation subsidy program promoted by the European Commission in 1992 could have acted as an initial source of *Phytophthora cinnamomi* infection. These findings together with the consideration of the spatial and temporal scale of the spreading are essential when planning the management of oak decline in open woodlands.

Keywords: *Phytophthora cinnamomi*; Dehesa ecosystems; Multivariate Adaptive Regression Splines; InhomogeneousRipley's K-function; Afforestation; Disease spread.

1. Introduction.

Oak open woodlands cover in the Iberian Peninsula 3,956,000 ha (Costa et al., 2006), accounting for7% of the total area. This ecosystem, known as "*Dehesa",* is mainly composed of Holm oak (*Quercus ilex*) and Cork oak (*Quercus suber*) combined with pastures in a savanna-like agroforestry system. *Dehesas* are considered to be one of the most biodiverse and multifunctional ecosystems (Martín et al., 2001; Díaz et al., 2003; Plieninger and Wilbrand, 2001; Moreno and Pulido, 2009; Bugalho et al., 2011) and are known to provide multiple ecosystem services (e.g.pasture and acorn for livestock, cork production or biodiversity conservation).

Oak decline has been reported in European forests since the beginning of the 20th century, becoming especially serious and widespread from the 1980s (Jung and Blaschke, 2000; de Sampaio e Paiva Camilo-Alves et al., 2013). It endangers the sustainability of both Iberian dehesas and associated ecosystem services, being therefore of major concern for farmers, forest managers and government institutions alike.

A range of biotic and abiotic factors as insects, fungi, drought, and other stress factors have been discussed as causes and predisposing factors of oak decline (Thomas et al., 2002). However, as Jung et al., (2018) state, these factors by themselves account for local and regional decline episodes rather than a worldwide phenomenon. Researches conducted since the early 1990s have suggested the oomycete *Phytophthora cinnamomi* Rands. as the main cause of oak decline in Mediterranean forests and open woodlands (Brasier, et al., 1993; Braisier, 1996; Gallego et al., 1999; Sánchez et al., 2002; Sánchez et al., 2003; Moreira and Martins, 2005; de Sampaio e Paiva Camilo-Alves et al., 2013; Linaldeddu et al., 2014). This soil-borne oomycete has been recognized as one of the most devastating plant pathogens in the world (Luque et al., 2014; Hardham and Blackman, 2018, Burgess et al., 2017; Sena et al., 2018). It affects a wide range of trees and shrubs, some of them of key economic and ecological importance such as oaks (*Quercus sp.*), eucalyptus

(Eucalyptus sp.), chestnut trees *(Castanea sativa)*, and avocado *(Persea americana)* (Zentemeyer, 1980; Braisier, 1996; Cahill et al., 2008; Ploetz, 2013; Jung et al., 2017), amongst others.

Oak decline processes are expected to become more frequent and virulent due to additive stress effects caused by increased temperature and drought periods driven by underlying climate change trends. These climatic patterns could also enhance the incidence of *Phytophthora cinnamomi* (Braisier, 1996; Sánchez et al., 2002; Bergot et al., 2004;de Sampaio e Paiva Camilo-Alves et al., 2013;Natalini et al., 2016; Duque-Lazo et al., 2018; Sena et al., 2018)

The study of spatio-temporal patterns of oak decline spreading at landscape level, although essential to articulate effective management and control measures (Holdenrieder et al., 2004; Moreira and Martins, 2005; Costa et al., 2010; Peterson et al., 2014; Sena et al., 2018; Duque-Lazo et al., 2018), has not received much attention. Landscape studies regarding the spatial patterns of the disease progression are needed to understand the influence of external factors acting on invasion and spreading processes further than local contagion (Ristaino and Gumpertz, 2000; Abellanas et al., 2017; Sena et al., 2018). Temporal analyses at landscape level could allow to assess the influence of changes in environmental factors on proneness to disease (i.e. management practices or changes in plant cover) (Holdenrieder et al., 2004) and also to weigh up the role of contagion (epidemic phenomenon) and new invasions (endemic issues) in disease spreading (Meyer et al.,2017). Studies at tree- and stand-level analyzing the influence of site factors have been carried out in Spain and Portugal (Sánchez et al., 2002; Moreira and Martins, 2005; de Sampaio e Paiva Camilo-Alves et al., 2013). These studies have shown significant relationships between some site variables (e.g., aspect, slope, and soil water content) and oak mortality caused by *Phytophthora* spp. (de Sampaio e Paiva Camilo-Alves et al., 2013; Cardillo et al., 2018). Wilson et al., (2003) studied the relationship of a wide range of variables with *Phytophthora cinnamomi* presence in vegetation communities from Australia to develop a predictive model. The results showed a negative association with elevation and positive with sun-index. In general, the local relationships obtained from tree level studies cannot be extrapolated to landscape analyses due to the complexity of the landscape and the multiple factors involved in the spreading. Studies at landscape-level focused on the forest disease named *sudden oak death*, caused by *Phytophthora ramorum,* have shown the relationship between dead trees and landscape variables (e.g., forest edge). Some studies have reported spatial aggregation patterns in *Phytophthora ramorum* foci over time (California and Oregon, USA) (Kelly and Meentemeyer, 2002; Liu et al., 2007).

Within the context of open woodland ecosystems, Abellanas et al., (2017) and Cardillo et al., (2012) addressed the spatial patterns of oak decline in Spanish *dehesas*. Both studies found statistical relationships between affected oaks and their proximity to roads whereas Cardillo et al., (2012) found affected trees to be correlated to their proximity to watercourses. Spatio-temporal studies expanding the analysis to further factors not considered in previous studies (e.g., geomorphology or management practices) are required to better understand spread patterns. Here, we address the study of oak decline patterns at landscape level considering the possible influence of a wide range of landscape descriptors, the interaction among affected trees and the temporal evolution of the decline process.

The aim of this study is to enhance and advance our understanding of the spatio-temporal patterns of oak decline at landscape level in *dehesa* ecosystems. This is achieved through two overarching objectives and their interpretation within the context of disease management:

(i) To characterize the spatial patterns of affected trees.

(ii) To study the potential role of a set of landscape descriptors in the spread of oak decline in three surveyed years (2001, 2009 and 2016).

2. Methodology

Affected trees and healthy spots (points randomly extracted from areas covered by healthy trees) from 2001, 2009 and 2016 were identified and geolocated in "El Andevalo" Region (Huelva, Spain. **Figure 1**). A spatial analysis using inhomogeneous Ripley's K-function was conducted to assess the spatial patterns of affected trees within years (univariate) and between years (bivariate). The association of oak decline with a set of potential predisposing factors the three years of study (2001, 2009 and 2016) was investigated implementing the non-parametric data mining technique Multivariate Adaptive Regression Splines (MARS).

2.1. Study area selection

“El Andevalo” (Huelva, Spain) is an area characterized by a sequence of rolling hills and plateaus. The average altitude along the area is150 m.a.s.l.“El Andevalo”’ has long and dry summers typical of the Mediterranean climate. The annual average precipitation is 550 mm, and the average temperature 17ºC. Lithology is characterized by eutric cambisols, eutric regosols, and lithosols with rankers (climatic and lithologic data from REDIAM, 2018). The land cover is dominated by *dehesas*, recent afforestations, and arable lands, with livestock farming systems and cereals production being the dominant land uses within the area. The

afforestations were established mainly during the second half of the ‘90s promoted by the subsidy program 1992 EEC Regulation 2080/92by the European Commission in 1992 (Jiménez and Navarro, 2014) aiming to convert agricultural lands into forested ones.

The study area was selected based on well documented evidence of significant oak decline presence in the zone (Carrasco, 2009). Small foci appeared in the early ‘90s with research studies carried out in 1998 and 2000 isolating*Phytophthora cinnamomi* from soil samples surveyed in farms from this area (Sánchez et al., 2002; Sánchez et al., 2003). Inside this region, the study area was defined by the *dehesa* covered areas (shape-file layer with the spatial distribution of *dehesa* areas from 1999, REDIAM, 2018)following the work by Abellanas et al., (2017). The analyses were carried out in this delimited *dehesa* area covering a total of 35,356 ha inside a total area of about 110,250 ha (45 km x 24,5 km)(**Figure1**).

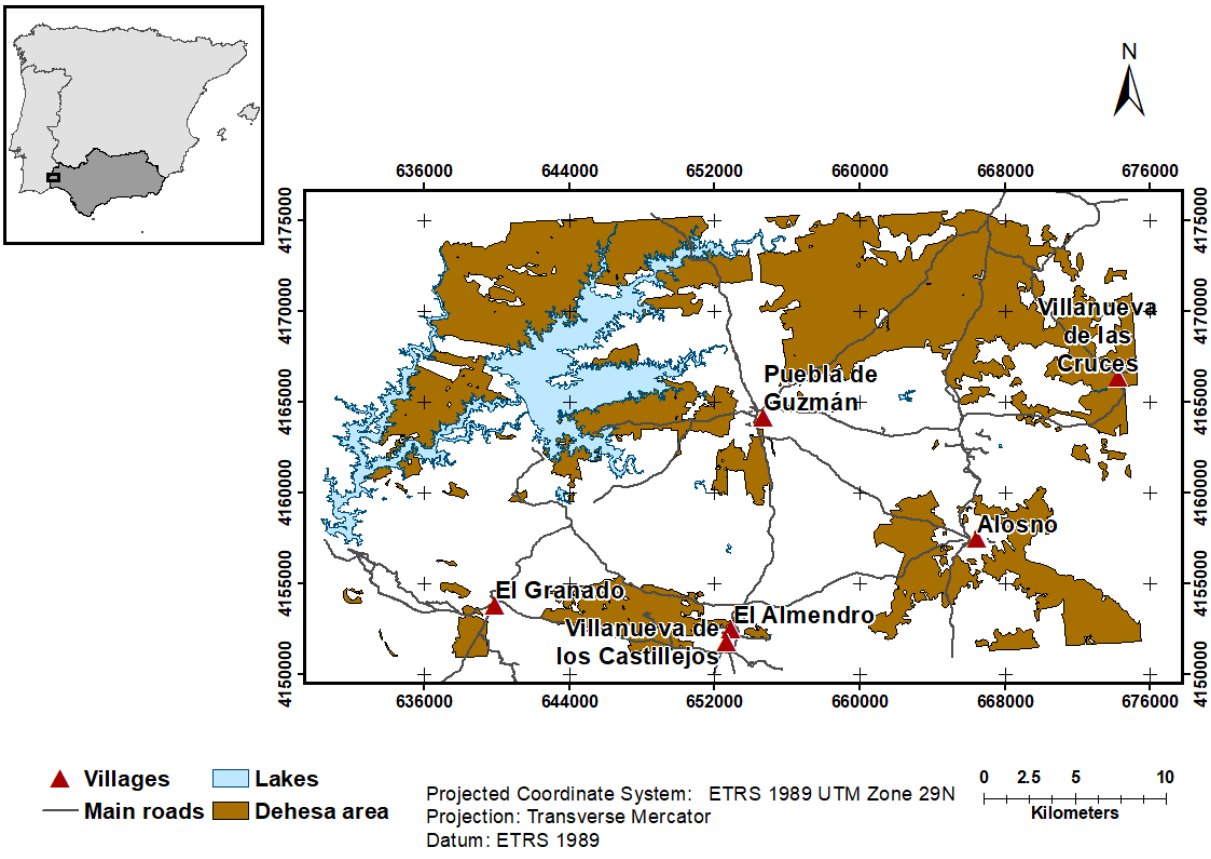

Figure 1. Location of the study area in El Andevalo region. The study area matches the *dehesa* area of the region (brown), delimited by a shape file layer of the spatial distribution of *dehesa* areas from 1999 (REDIAM, 2018).

2.2. Identification of affected and healthy trees.

Aerial orthophotography at 0.5 m resolution collected in 2001 (July), 2009 (April-May) and 2016 (July) (Linea,2018) were photo-interpreted to identify trees affected by oak decline. The imagery was visually inspected by trained operators and all trees affected were identified based on partial or total defoliation(**Figure 2, A and B**; Abellanas et al., 2017; Cardillo et al., 2012). Oak decline in Mediterranean forest is characterized by progressive crown thinning, branch dieback and defoliation (Jung et al., 2018), although the range of symptoms could be highly variable within the same area (Gallego et al., 1999; Moreira and Martins, 2005; de Sampaio e Paiva Camilo-Alves et al., 2013).

It is not unusual in the zone that clustered trees are the same individual, sharing a unique rootstock, coming from ancient coppicing or root sprouts. For this reason, a buffer circle was associated with each affected tree and it was considered as *affected spot*. The size of the affected spot was established to exceed the area occupied by the roots of the affected tree. Dinis (2014) showed that, in dehesa, superficial oak roots can spread away at least two times the canopy projection for the majority of the directions (azimuths), reaching in some cases a maximum distance of four times the canopy projection. The average crown diameter of oak trees in this area was 8.9 $\pm$ 0.06 m (Fernández-Rebollo et al., 2017), therefore the buffer distance turned out to be between 8.9 m and 17.8 m. Finally, a buffer area of 15 m radius was chosen (**Figure2.B**). Affected trees falling within the 15m-buffer of the central affected one were not tagged as different ones to ensure that sprouts of the same tree were not counted as additional individuals. Affected spots showing symptoms of oak decline within livestock enclosures and also those closer than 15 meters to water bodies, were excluded from the analysis as their cause of death could be attributed to other local causes not linked to general oak decline episodes at landscape level(Cardillo et al., 2012; Abellanas et al., 2017).Management practices of Holm and Cork oak trees that could lead to misclassification with (**Figure 2.C**) were also considered during the identification of affected spots.

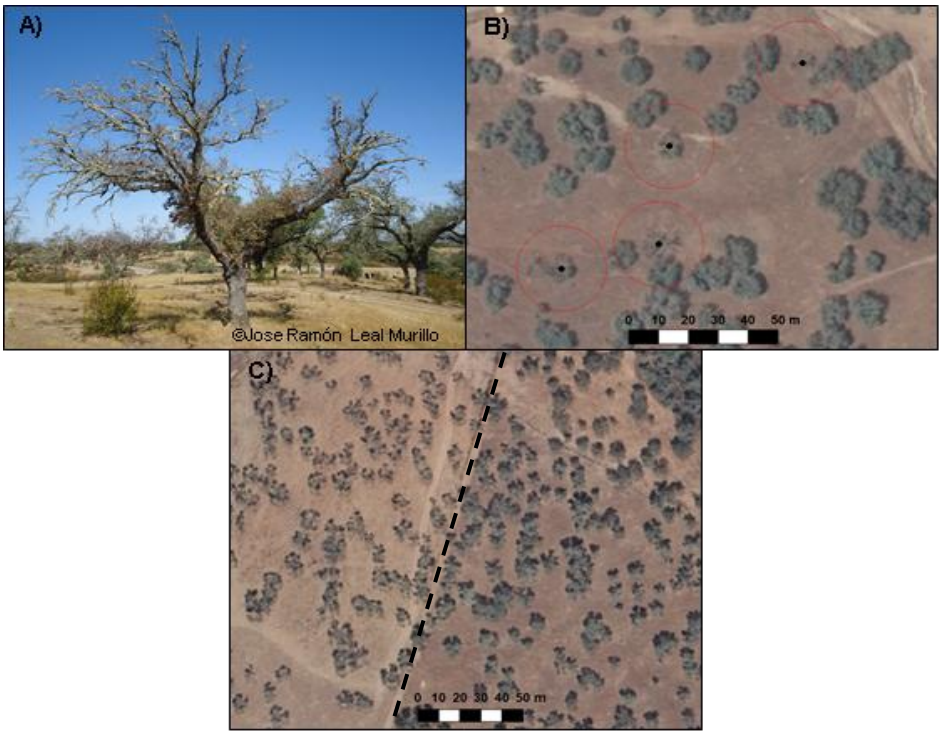

Figure 2.A) Affected Holm oak by *Phytophthora cinnamomi* in El Andévalo region in 2009 showing evident defoliation. **B)** Spots affected by oak decline identified in El Andévalo in orthophoto from 2009. **C)** Left; Field with pruned trees showing similar appearance to defoliated trees due to oak decline. Right; Different field where trees have not been pruned (2009, El Andévalo).

The accuracy in affected spots detection was assessed based on recognition of the status of affected spots in the following dates. The status (healthy/affected) of each spot considered as affected within the 2001 sample was identified in the 2009 imagery. Those that have not shown any symptoms in 2009 were considered to have been erroneously classed as affected in the previous date. Within the area, cutting dead trees is a common practice (Sánchez et al., 2002); affected trees identified in 2001 but not present in the 2009 imagery were considered to have been cut and were classified as truly affected trees in 2001. The same approach was used for 2009 regarding 2016 status. It was assumed that affected trees do not recover from the disease (Brasier, 1996). Percentage values of misclassification were assessed from a sample of affected spots *n* equal to 354 (2001) and 368 (2009) for 95% confidence (Z=1.96) and 5% error (E=0.05), p=0.5, q=0.5 (being p and q the probabilities of success and failure, respectively) and N=total number of affected spots in each year in equation (1). From sampled spots classified as affected in 2001, 79% were classified as dead in 2009, 16% as symptomatic and only 5% were classified as healthy, being this figure the estimated error of observations in 2001. In 2009 a similar error figure was estimated: 84% of sampled spots classified as affected in 2009 were classified as dead in 2016, 12% as symptomatic, and 4% as healthy trees, being this figure the estimated error for 2009.

$$n = \frac{(NZ^2qp)}{\left((N-1)E^2 + (Z^2pq)\right)} \quad (1)$$

Even if the studied disease could affect other species, the main ones affected and those of our interest are the tree species in the dehesa, so for our purpose, we assume that the disease inhabits only on the trees. It was necessary, then, to estimate the susceptible area of infection as the tree-covered area among the entire study area, since we are dealing with open forests. The tree-covered area was identified using an object-based classification developed with the Example-Based Classification module from ENVI 5.4. For that purpose, RGB aerial photography from 1998 at 1 m resolution was used to ensure the whole tree-covered area pre-2001 was captured. From this previous tree-covered area we derived "healthy-tree-covered areas" for each study date by subtracting the affected spots identified each date (15m radius buffer around each affected tree) from the previous "healthy tree-covered area". From these shrinking healthy area, we successively randomly selected "healthy spots" whose central points were used to compare with affected spots. We used the same number of spots as the number of identified affected spots each year (Baddeley, 2014).

This data set of healthy and affected spots, converted to points (each spot represented by its central point), constituted the presence/absence data to fit the MARS models. Affected spots were also used for the analysis of spatial patterns of dispersion with inhomogeneous Ripley´s K-function. Since the objectives of the subsequent analyses were to characterize the spatial patterns of spread of oak decline and relations with landscape descriptors (MARS) in different years, those spots recorded as affected in previous years were excluded in the successive years, so only the newly affected spots were considered in each date.

2.3. Extraction of landscape descriptors

A total of ten landscape descriptors known to affect oak decline (Kelly and Meentemeyer, 2002; Wilson et al., 2003; Cardillo et al., 2012; de Sampaio e Paiva Camilo-Alves et al., 2013; Abellanas et al., 2017; Peterson et al., 2014) were derived from available geographic data (**Table 1**). The first five topographic descriptors: ASPECT (compass direction -N, NE, E, SE, S, SW, W or NW- that the pixel faces in this location), SLOPE (slope gradient of each pixel calculated by the average maximum technique according Burrough and McDonell, 1998), ELV (Elevation) , FLOWAC (Flow Accumulation) and TMI

(Topographic Moisture Index) were extracted from a 5 m resolution Digital Elevation Model (DEM) from 2015 (IGN, 2018) using the following available tools in ArcMap 10: Aspect, Slope and Flow Accumulation (ESRI, 2016). The procedure to derive the Flow accumulation in ArcMap follows the methodology presented in Jenson and Domingue(1988), by which the derived value for a raster pixel represents the number of pixels flowing downslope into this pixel. A threshold value of 50 pixels was set to avoid bias caused by pixels falling in rivers, which could derive to extreme values. This threshold value was selected by comparing the flow accumulation values with the stream network used to represent watercourses for deriving variable WATER (Minimum distance to watercourses). Following the approach of Kelly and Meentemeyer (2002), the TMI was calculated according to Moore et al., (1991):

$$\mathrm{TMI} = \ln\left(\frac{a}{\tan b}\right) \quad (2)$$

Where *a* is the upslope drainage given by the calculated flow accumulation (FLOWAC) and *b* represents the slope gradient. The extracted values were normalized.

The values of these five variables at the location of the affected and healthy spots were extracted from the raster by *Extract Multi Values to Points* tool. The distance to features of the landscape was calculated with *Near* tool also from ArcMap 10.5. It represents the minimum distance from an affected/healthy spot to the closest corresponding feature, lines for ROADS and WATER, and the edge of the polygon for RESEV (Minimum Distance to reservoirs), REFOR (Minimum Distance to Afforested patches) and URBAN (Minimum distance to Urban polygons). For affected/healthy spots falling within the polygon, the distance is 0 m. Descriptive statistics of the extracted values of the variables are shown in **Table 2.**

Data for the landscape descriptors that have suffered some changes over time (mainly those linked to human activities) were derived based on the closest (in time) data source available (**Table 1**). Regarding REFOR, the main reforestation activity in the region spanned from 1994 to 2001, but most of the affected land was reforested during the first half of the period; more than 75% was carried out between the years 1995 and 1998, and by the year 2000, a year before our first study date, more than 95% of the reforestation was already completed, so the reforested polygons considered to define the variable REFOR were the same for all the study dates. The Andalusian Administration responsible for the afforestation program provided the shape-files containing the forested polygons.

Table 1. Landscape descriptors considered for data analysis (REDIAM, 2018)[1]. (IGN, 2018)[2]. Regional Ministry of Agriculture, Fishing and Rural Development of Andalusia (JA)[3]. "Year" refers to the year for which the data source was available. S.R.: Spatial Resolution (m)

Landscape descriptors	Code	Units	Year	Source	S.R.
Aspect	ASPECT	categorical	2015	DEM[2]	5
Slope	SLOPE	degrees	2015	DEM[2]	5
Elevation	ELV	m	2015	DEM[2]	5
Flow accumulation	FLOWAC	N pixels	2015	DEM[2]	5
Topographic moisture Index	TMI	dimensionless	2015	DEM[2]	5
Distance to roads	ROADS	m	2009	IGN[2]	3
Distance to watercourses	WATER	m	2009/2016	IGN[2]	3
Distance to afforestations	REFOR	m	2011	JA[3]	5
Distance to urban areas	URBAN	m	2005/2009/2013	Land use map[1]	5
Distance to reservoirs	RESEV	m	2005/2009/2015	Land use map[1]	5

2.4. Spatial analysis of affected spots.

Spatial patterns of oak decline spread within the study area were quantified using Ripley's K-function (Ripley, 1977). To perform this analysis, the coordinates of the central point of affected spots previously identified were extracted. Ripley's K-function is a second-order characteristic widely used to assess spatial patterns at multiple scales in forests and plant ecology (Szwagrzyk and Czerwczak, 1993; Haase, 1995; Vacek and Lepš, 1996; Eccles et al., 1999; Getzin et al., 2008; Liu et al., 2014; Fibich et al., 2016). The function has been successfully applied to characterize spatial patterns of sudden oak death caused by *Phytophthora ramorum* (Kelly and Meentemeyer, 2002; Liu et al., 2007).

Given a point pattern with intensity λ, the K-function defined as $\lambda K(r)$, represents the expected number of points located within a distance (r) of a random point of the pattern (Ripley, 1977). For bivariate point patterns, where two types of points, i and j, share the space, K-function represents the number of points of type j within a distance r of a random point of type i, divided by the intensity λ_j of the pattern of points of type j (Wiegand, 2004). The K-function relies on the assumption that the point process is homogeneous (i.e., stationary and isotropic). Spatial trends and covariates of the point patterns could lead to non-spatially-constant intensity, this indicating inhomogeneous processes(Brodie et al., 1995; Liu et al., 2007; Lin et al., 2011). Liu et al. (2007) found better point pattern description when the spatial patterns of sudden oak death are considered as inhomogeneous. As the here studied affected trees intensity is expected to vary due to covariates (e.g., factors driving the initiation of the disease), the point processes were assumed to be

inhomogeneous and the inhomogeneous K-function was applied (**Eq. 3a**) (Baddeley et al., 2000). This assumption ensured that the observed spatial interactions were not influenced by spatial variation of the intensity function (Liu et al., 2007). The notation for the inhomogeneous K-function is as follows:

$$K_{\text{inhom}}(r) = \frac{1}{R}\sum_{i=1}^{N}\sum_{j\neq i}\frac{w_{ij}I(d_{ij}\leq r)}{\lambda(s_i)\lambda(s_j)} \quad (3a)$$

Where *R* represents the study area; w_{ij} is an edge correction factor; N is the total number of affected trees (points); $\lambda(s_i)$ and $\lambda(s_j)$ the intensity function values at points s_i and s_j; d_{ij}, distance between s_i and s_j; $I(d_{ij}\leq r)$ equals to 1 if $d_{ij}\leq r$, 0 otherwise.

The dependency between pairwise affected spots patterns from different years was quantified via bivariate analysis of marked point patterns, being the year the point's mark (Baddeley, 2010). For that purpose, the generalized K-function, called inhomogeneous cross-K-function for bivariate inhomogeneous processes (Liu et al., 2007), was applied (3b).

$$K_{\text{inhom}}(m,n;r) = \frac{1}{R}\sum_{i=1}^{N_m}\sum_{j=1}^{N_n}\frac{w_{ij}I(d_{ij}\leq r)}{\lambda_m(s_{m,i})\lambda_n(s_{n,j})} \quad (3b)$$

Where R represents the study area; w_{ij} is an edge correction factor; N_m and N_n are the total number of newly affected trees in years m and n, respectively; $d_{i,j}$ is the distance between point $s_{m,i}$ of year m and point $s_{n,I}$ of year n; $\lambda_m(s_{m,i})$ and $\lambda_n(s_{n,j})$ are the values of intensity functions of point patterns of years *m* and *n* at points $s_{m,i}$ and $s_{n,j}$, respectively; $I(d_{ij}\leq r)$ equals to 1 if $d_{ij}\leq r$, 0 otherwise.

To facilitate the interpretation and visualization of K_{inhom} and *cross-*K_{inhom} the normalized function proposed by Besag, (1977) was applied:

$$L_{inhom} - r = \sqrt{\frac{K_{\text{inhom}}(r)}{\pi}} - r \quad (4)$$

This function is used to investigate the departure from randomness of the point patterns in the case of its univariate form, and the independence between points of different types in the bivariate form. For univariate point patterns, values of L(r)-r close to zero for every r indicate randomness, while values greater than zero mean clustering patterns and values lower than zero are sign of overdispersed points. For bivariate point patterns, L(r)-r

equal zero means spatial independence between points of different types, being values greater than zero indication of attraction among points of different types at distance r, and, conversely, values lower than zero mean repulsion of points of different types.

The analysis was implemented using “spatstat” / “earth” Rpackage in R studio (v. 1.1.453) following Baddeley et al., 2018. To correct the edge effect of Ripley's K-function (Haase, 1995), the border method or “reduced sample”(Ripley, 1991) was applied due to its computational efficiency and suitability when dealing with non-geometrical windows (Baddeley et al., 2018). Statistical significance and confidence intervals of Ripley's K-function are commonly tested using Monte Carlo pointwise simulations envelopes. However, this method is valid as exploratory analysis but it cannot be used to define the level of significance (Loosmore and Ford, 2006; Baddeley et al., 2014; Velázquez et al., 2016). As Velázquez et al.,(2016) recommended, the statistically valid test global envelope (Myllymäki et al., 2017) was used to test the null hypothesis of random distribution. Using this test, the confidence intervals to assess the significance of the departure from Inhomogeneous Poisson Process (IPP) were created through the generation of 99 simulations ($\alpha = 0.02$) of IPP.

In order to gain spatial visibility at landscape level, a graphical approach was also tackled using the kernel density tool of ArcMap to produce a map of density of affected trees in the whole studied area. This tool computes a magnitude per unit area for each raster cell (density of affected trees) using a kernel function to fit a smoothly tapered surface to each point, assigning then a density to each pixel of the area by adding the volumes under all kernel surfaces that overlap the pixel center.

2.5. Analysis of landscape descriptors using MARS

Multivariate Adaptive Regression Splines (MARS; Friedman, 1991) was used to investigate the relationship between landscape descriptors (explanatory variables) and oak decline. MARS is a non-parametric flexible regression modelling method that has shown its suitability when dealing with a high number of variables, collinearity, complex non-linear and linear relationships between predictors and response, allowing easier interpretation of results than similar methods (De Veaux et al., 1993; Muñoz and Felicísimo, 2004; Sharda et al., 2008;Gómez Gutiérrez et al.,2009a; 2009b; Herguido et al., 2017a). MARS produces a regression line that is allowed to bend at certain knots or nodes that mark a change in the behavior of the function. These knots mark the start and end of functions called basis functions (BFs). BFs represent either, linear or non-linear relationship between response and

the most determinant predictors at this section of the regression (Muñoz and Felicísimo, 2004). The equation is described as follows:

$$y = f(x) = \beta_0 + \sum_{m=1}^{M} \beta_m h_m(x) \quad (5)$$

where y is the predicted value, $f(x)$ the MARS's function, β_0 represents an initial constant, M is the sum of terms and β_m and $h_m(x)$ the coefficient and BFs of each of these terms.

The MARS analysis approaches the response to a constant (β_0) and then establishes the knots through a forward pass that determines all the possible BFs. Because of the forward pass, an overfitted model is generated. Then, a backward or pruning pass selects the most important BFs (those with the lowest residual sum of squares; RSS). The output of the forward pass is a sequence of models or subsets of the overfitted model with different numbers of BFs. To select the best model, MARS calculates the Generalized Cross-Validation (GCV; Craven and Wahba, 1978) and chooses the model with the lowest GCV value (Gómez Gutiérrez et al., 2009a; Herguido et al., 2017a). The "earth" R package in R studio (v. 1.1.453) was used to perform MARS (Milborrow, 2018b). The generalized cross-validation expression (GCV; Craven and Wahba, 1978) is as follows:

$$GCV(M) = \frac{1}{N} \frac{\sum_{1=1}^{N} (y_i - f_M(x_i))^2}{(1 - \frac{C(M)}{N})^2} \quad (6)$$

where M is the number of terms, N the number of cases, y the dependent variable, $f_M(x_i)$, the value given by the model and $C(M)$ a cost function for this number of terms.

The model outputs were validated via cross-validation. For that purpose, the dataset was randomly divided into five folds. Five validation models were built leaving, each time, one of the five folds apart for testing and using the other four for training. This way, five measures of R^2 of the predictions were made. Following the recommendation of Milborrow (2018a), this process was repeated 3 times to average out the variation, ensuring more stable results. The final result of the cross-validation is the average of R^2 values thus obtained denoted by CVRsq.

The dependent variable introduced in MARS was binary presence/absence data (0: healthy spot; 1: affected spot). The same number of observations was used for both healthy and affected spots. The landscape descriptors constituted the model predictors (**Table 1**).

Based on Leathwick et al., (2005), a generalized linear model (GLM; McCullagh and Nelder,1989) was included in the MARS algorithm to fit the final binomial MARS model; the GLM is invoked after the backward pass (Milborrow, 2018a).

Models' performance from each year was assessed via the Receiver Operating Characteristic (ROC) and the Area Under the Curve (AUC) (Swets, 1988; DeLeo, 1993; Fielding and Bell, 1997; Pearce and Ferrier, 2000; Gómez Gutiérrez et al., 2009a; Herguido et al., 2017a). ROC provides a measure of the capacity of the model to discriminate between presence/absence of the dependent variable (healthy spots/affected spots). To do that, ROC represents sensitivity (true positives) against specificity (true negatives). The closer the ROC curve is to the upper-left side of the graph, the better is the performance of the MARS model. AUC should be close to 1; areas above 0.7 are commonly considered as acceptable discrimination and model performance, but this threshold could be lower in cases of unbalanced prevalence. In any case, an AUC of 0.5 following the 45º line means no discrimination ability of the model (Swets, 1988; Fielding and Bell, 1997; Pearce and Ferrier, 2000). The significance of MARS models was tested by the use of null-models (Raes and der Steege, 2007). For each year, 99 null-models were run by randomly drawing from the study area the same number of virtual presence/absence localities than for the empirical models. A model is considered as significantly different from random expectation if its AUC value exceeds the 95% quantile of the 99 null-model AUC values.

To interpret the role of each variable, MARS allows the estimation of the relative importance (RI) of the variables included in the model. This measure of importance reflects the strength of the relationship between the predictor variables and the response (Milborrow, 2018a). To estimate the RI, during the backward pass, RI measures the relative decrease of the residual sum of square (RSS) for each subset in relation to the previous one. Then, the sum of the decreases overall subsets are scaled to the largest value (so the most important variable accounts for 100% RI). Those variables that give larger RSS' decreases through the subsets are considered to be more significant (Milborrow, 2018a). Additionally, MARS estimates the RI based on the number of subsets that include a certain variable; the more subsets include a variable, the more important this variable is. MARS excludes automatically those variables that are not relevant for the discrimination of the classes in the dependent variable.

Following the approach of Herguido et al., (2017a), in order to make the interpretation of the relationships between variables and outcomes easier, the Spearman correlation

coefficients between the continuous predictor variables and the values predicted by the models were calculated.

3. Results

3.1. Identification of affected spots and selection of healthy spots

A total of 4,521 affected spots by oak decline were identified in the year 2001; 8,632 in the year 2009 and 28,617 in the year 2016 (**Figure 3**). The Kernel density maps confirm the exponential increase of accumulated affected spots (see Fig. SM1 in Supplementary Material),showing clustering of affected spots in four hot spots in 2001 whose density increase from less than 100 affected spots/km^2 to more than 400 affected spots/km^2 in 2016, reaching 735 affected spots/km^2 in the northern part of the study area. The increment of affected spots is consistent in the same hot spots over the three years.

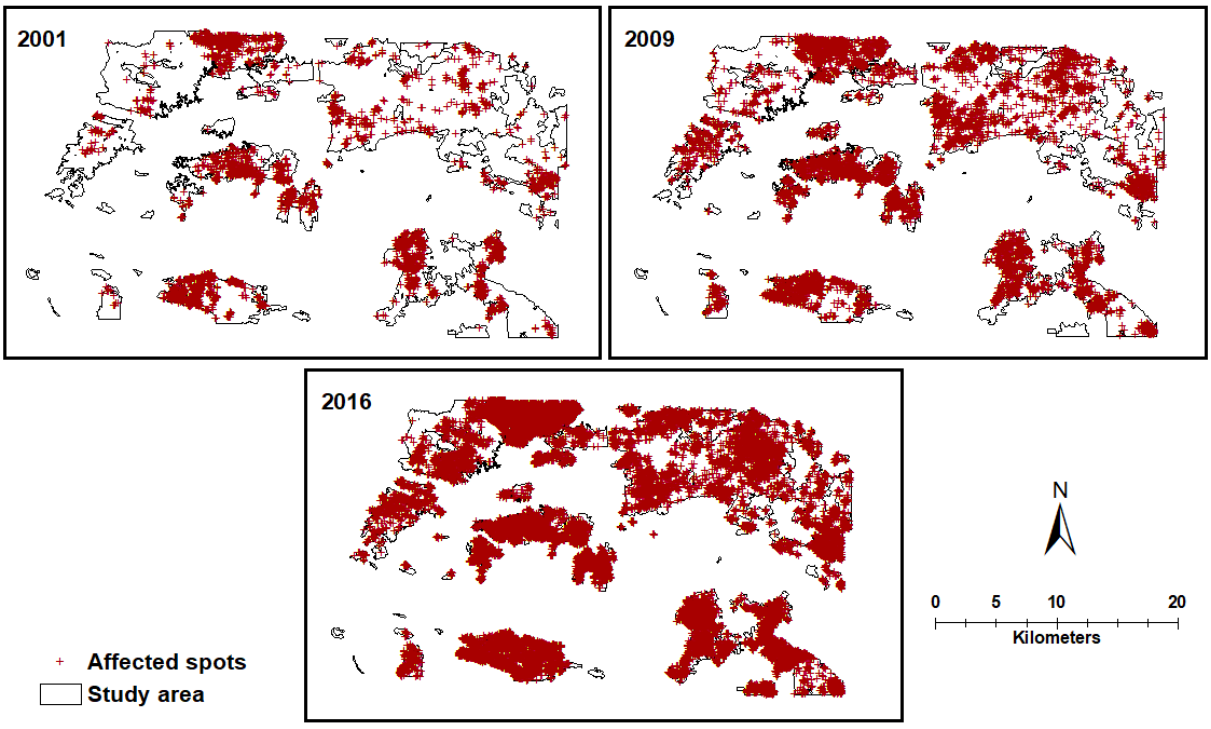

Figure 3. Newly affected spots (oak decline)identified through photo interpretation for the study area (*Dehesa* stands in El Andévalo region) in each individual year.

From the RGB aerial photography from 1998 at 1 m resolution, a shape with the initial "tree-covered area" was obtained via object-based classification rendering a tree-covered surface of 13,073.17 ha out of the 35,356 ha total surface of the study area

(See Fig SM3 in Supplementary Material). The validity of this classification was assessed via a confusion matrix, which reported an overall accuracy of 77%. From this previous tree-covered area we randomly selected "healthy spots", avoiding the affected spots previously identified. We selected the same number of spots as the number of identified affected spots each year n=4,521 for 2001; n=8,632 for 2009; and n=28,617 for 2016

3.2. Landscape descriptors statistics

The descriptive statistics of the extracted values of landscape descriptors for 2001, 2009 and 2016 are shown in Table 2. For the categorical variable ASPECT, the frequency of the classes is reported. Overall, all the variables but TMI and FLOWAC show lower means for affected spots than for healthy spots. TMI shows the opposite trend while FLOWAC does not show constant trends. Frequency values of ASPECT do not present any trend. The CV values seem to be especially high for FLOWAC, with values over 1 in all years for both, healthy and affected spots. Table SM1 (Supplementary Material) shows the p values for the ANOVA or Welch's unequal variance t-test run each study date. Variables were transformed when necessary to gain homoscedasticity or Welch's two-sample t-test, that is robust to the departure from it, has been used. Density functions of the main descriptors for affected and healthy spots can be seen in Fig. SM2 in Supplementary material.

Table 2. Summary statistics (average values, CV in brackets) of landscape descriptors of affected and healthy spots. ELV (m), SLOPE (degrees), FLOWAC (number of pixels), TMI (dimensionless), WATER (m), ROADS (m), REFOR(m), RESEV(m), URBAN(m), ASPECT (categorical).

a) Year 2001 (Number of Affected spots = Number of healthy spots=4,521)

	ELV	SLOPE	FLOWAC	TMI	WATER	ROADS
Affected	164.433 (0.203)	11.799 (0.534)	9.686 (1.368)	0.170 (0.309)	118.999 (0.771)	130.164 (0.828)
Healthy	163.731 (0.256)	15.593 (0.612)	8.713 (1.474)	0.159 (0.374)	137.706 (0.846)	157.029 (0.825)

	REFOR	RESEV	URBAN	ASPECT (Frequency %)			
Affected	647.701 (0.978)	374.142 (0.695)	1097.645 (0.563)	N=12% S=16%	NE=12% SE=14%	NW=11% SW=14%	E=11% W=10%
Healthy	760.187 (0.830)	419.370 (0.672)	1186.133 (0.689)	N=13% S=16%	NE=13% SE=12%	NW=12% SW=13%	E=11% W=11%

b) Year 2009 (Number of Affected spots = Number of healthy spots =8,632)

	ELV	SLOPE	FLOWAC	TMI	WATER	ROADS
Affected	163.873	12.526	8.692	0.164	129.764	131.423

	(0.221)	(0.530)	(1.430)	(0.310)	(0.852)	(0.827)
Healthy	164.397	15.520	8.995	0.160	136.161	159.331
	(0.255)	(0.611)	(1.455)	(0.374)	(0.855)	(0.849)

	REFOR	RESEV	URBAN	ASPECT (Frequency %)			
Affected	653.391	374.611	1008.150	N=13%	NE=12%	NW=12%	E=10%
	(0.942)	(0.711)	(0.720)	S=15%	SE=12%	SW=15%	W=12%
Healthy	762.316	425.158	1157.461	N=13%	NE=13%	NW=11%	E=12%
	(0.830)	(0.681)	(0.692)	S=14%	SE=12%	SW=13%	W=12%

c) Year 2016(Number of Affected spots = Number of healthy spots =28,617)

	ELV	SLOPE	FLOWAC	TMI	WATER	ROADS
Affected	163.716	13.694	7.967	0.159	127.298	143.692
	(0.235)	(0.537)	(1.492)	(0.322)	(0.829)	(0.830)
Healthy	164.787	15.704	8.878	0.159	137.615	157.254
	(0.257)	(0.612)	(1.488)	(0.382)	(0.853)	(0.833)

	REFOR	RESEV	URBAN	ASPECT (Frequency %)			
Affected	827.557	346.271	976.003	N=14%	NE=13%	NW=11%	E=11%
	(0.854)	(0.737)	(0.673)	S=13%	SE=11%	SW=14%	W=11%
Healthy	755.986	411.196	1112.696	N=13%	NE=13%	NW=11%	E=12%
	(0.820)	(0.691)	(0.739)	S=14%	SE=12%	SW=14%	W=11%

3.3. Spatial analysis of affected spots

For the three years, the univariate $L_{inhom}(r)$-r function clearly departs from spatial randomness indicating strong clustering. The scale of clustering is approximately 1,750 m and similar for the three years patterns. The dominant clustering distance represented by the r corresponding to the $L_{inhom}(r)$-r peak value is located at 1000m. and constant over the three years. Although the aggregation of affected spots is evident in all the three years, it decreases over the time and approximates to spatial randomness in 2016, when the $L_{inhom}(r)$-r function peak value reaches half of the value of 2001 (**Figure4**).

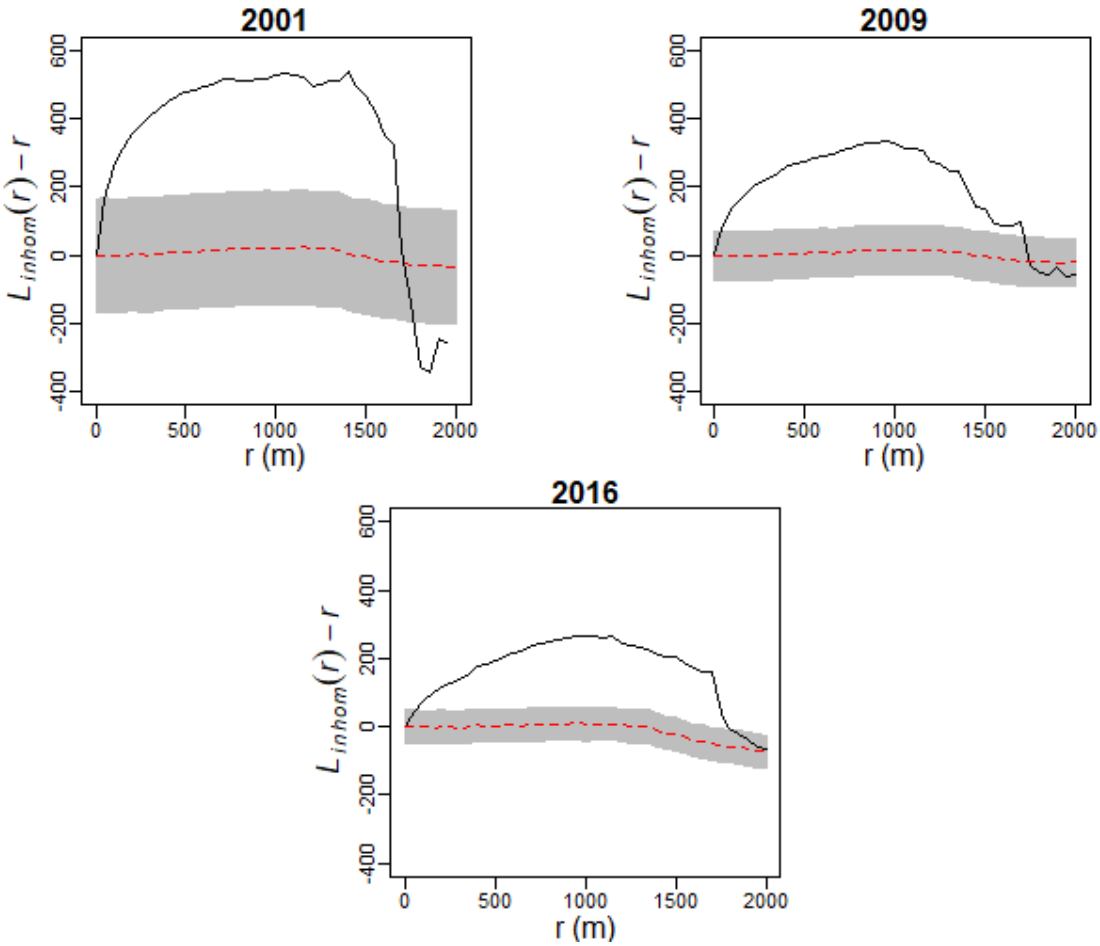

Figure 4. Normalized K functions of the univariate analysis of affected spots patterns from 2001, 2009 and 2016 assuming inhomogeneity. The solid black line represents the empirical $L_{inhom}(r)$-r function values, red dotted line corresponds to the theoretical function of the Inhomogeneous Poisson Process (IPP) and shaded areas are the 99 global envelope simulations (α= 0.02) of the IPP.

For the bivariate analysis, all the pairwise patterns exceed the 99 simulation envelopes (**Figure5**). This indicates a significant strong attraction between affected spots from different years. The scale of clustering for 2001 vs 2009 is 1500 m, while for 2009 vs 2016 and 2001 vs 2016 is approximately 1800 m.

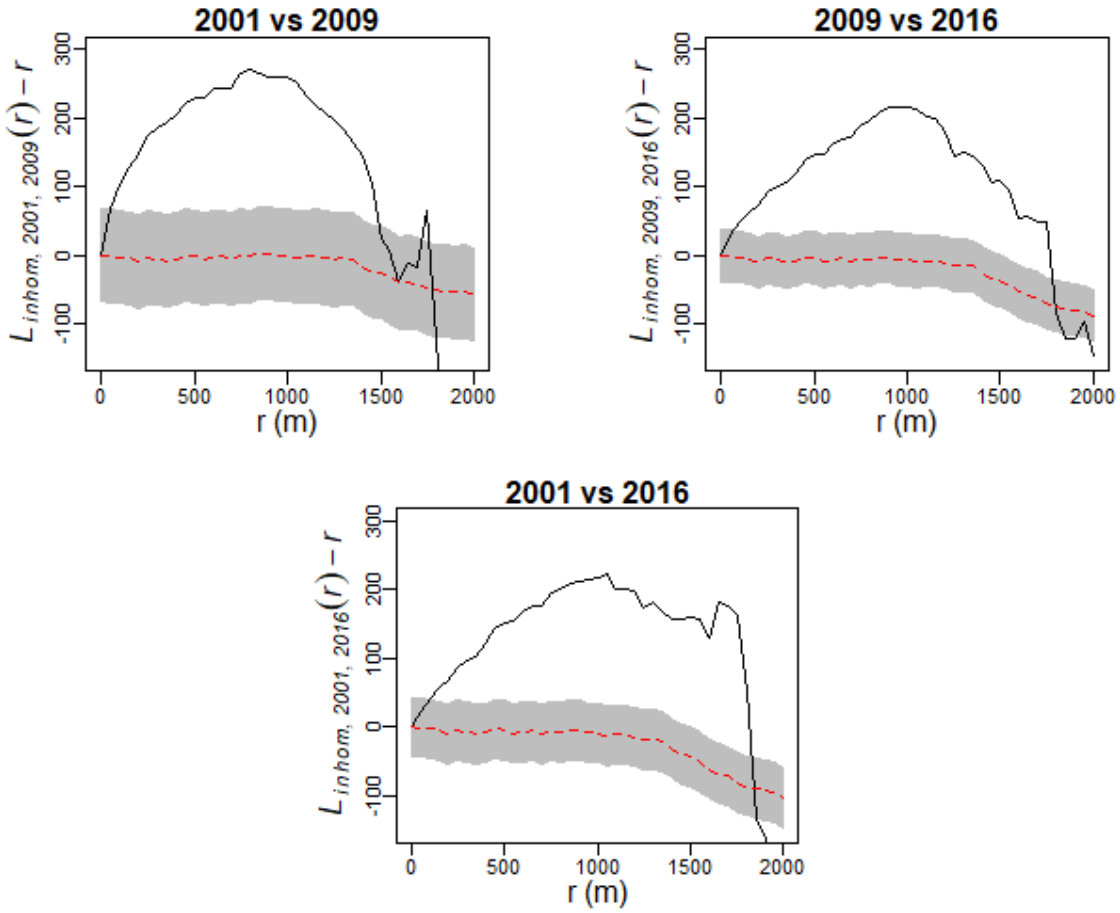

Figure5. Normalized cross-K functions of the bivariate analysis of pairwise marked point patterns of affected spots assuming inhomogeneity. The solid black line represents the empirical *cross-*$L_{inhom}(r)$*-r* function values, red dotted line corresponds to the theoretical function of the Inhomogeneous Poisson process (IPP) and shaded areas are the 99 global envelope simulations (α= 0.02) of the IPP.

3.4. Analysis of explanatory variables using MARS

The three MARS models are significantly different from random since their AUC values clearly depart from the 95% quantile of the 99 null-model AUC values**(Table 3)**. The AUC value in 2001 indicates a satisfactory fitting of the model (>0.7); the variables selected by the model have an important influence on the discrimination between healthy and affected spots. In the following study dates (2009, 2016), the AUC shows slightly decreasing values which could be an artifact due to the unbalanced prevalence of data derived from the increase in affected trees with the exponential progression of the disease over time (Raes and der Steege, 2007)(**Table 3** and **Figure6**).

Table 3. Statistics of Multivariate Adaptive Regression Splines models for 2001, 2009 and 2016. Area under the curve (AUC), 95% quantile of the 99 null-model AUC values (Null-models AUC 95% quantile), Generalized cross-validation (GCV), and mean of the out-of-fold R^2 values (CVRsq).

Year	AUC	Null-models AUC 95% quantile	GCV	CVRsq
2001	0.707	0.523	0.216	0.130
2009	0.671	0.500	0.226	0.093
2016	0.651	0.500	0.232	0.071

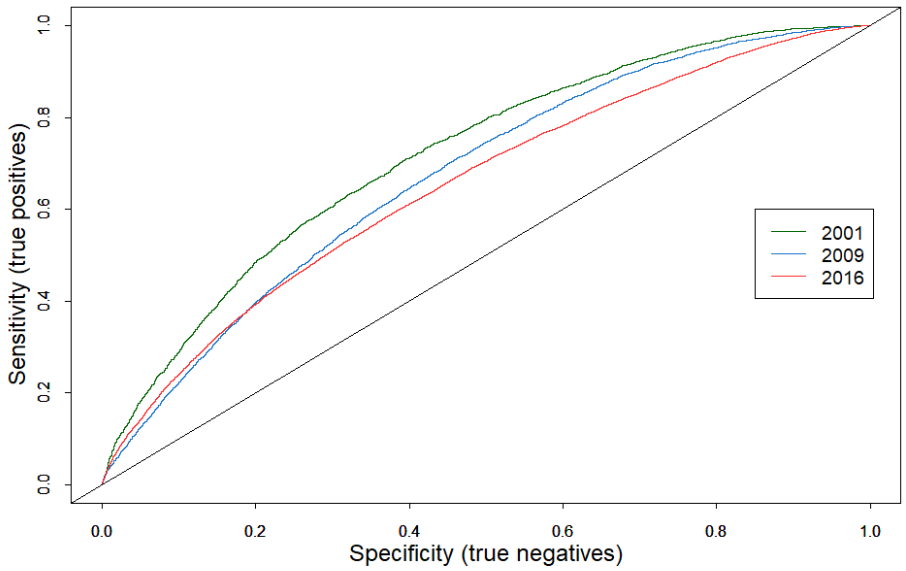

Figure6. Receiver Operating Characteristic curve of Multivariate Adaptive Regression Splines models from 2001, 2009 and 2016.

The results obtained for RI (**Table 4**) show that SLOPE was the most significant explanatory variable over the three years. REFOR showed high importance in 2001 and 2009 whereas in 2016 its relative importance decreased. The significance of WATER decreased from 2001 to 2009 and 2016 increasing that of other variables. However, URBAN presented constant values of importance along the three years taking the fourth place in 2001 and 2009 and third in 2016. ELV seemed to have intermediate importance over time. TMI occupied the bottom half position in order of RI for all the years. ROADS, which in 2001 was, after RESEV, the least important variable, became more important in 2009 and was excluded from the model in 2016. RESEV showed an increase in importance over time from the last position in RI in 2001 to the second most important variable in 2016. FLOWAC and ASPEC were excluded from all models, indicating that these variables were irrelevant in the

model to discriminate between healthy and affected spots. The order of RI was consistent with both criteria (decrease of RSS and the number of subsets) for the three models.

The Spearman correlation factors between predicted values and variables were significant in most cases (**Table 5**), showing that all the explanatory variables but TMI correlate negatively with the probability of spots being affected. Predicted values were extracted to compute the Spearman correlation coefficient factors to show the correlation sign, not for predictive purposes.

Table 4. Relative importance of landscape predictors in Multivariate Adaptive Regression Splines models for each year. RI stands for relative importance based on the relative decrease of the residual sum of square (RSS) and Nsubsets stands for the number of subsets in which the variable was included. "Unused" indicates that this variable was not relevant for the discrimination between affected and healthy spots.

	MARS model 2001			MARS model 2009			MARS model 2016		
Variables	**RI (%)**	**Nsubsets**	**Order of RI**	**RI (%)**	**Nsubsets**	**Order of RI**	**RI (%)**	**Nsubsets**	**Order of RI**
SLOPE	100.0	24	1/8	100.0	15	1/8	100	18	1/7
REFOR	78.1	23	2/8	78.8	14	2/8	33.6	7	7/7
WATER	71.8	22	3/8	39.7	8	7/8	37.9	8	6/7
URBAN	66.5	21	4/8	66.5	12	4/8	80.4	16	3/7
ELV	54.0	18	5/8	71.3	13	3/8	75.1	15	4/7
TMI	40.9	14	6/8	24.5	5	8/8	56.3	12	5/7
ROADS	27.6	10	7/8	52.8	10	5/8	unused	unused	-
RESEV	17.3	6	8/8	44.7	9	6/8	87.4	17	2/7
FLOWAC	unused	unused	-	unused	unused	-	unused	unused	-
ASPECT	unused	unused	-	unused	unused	-	unused	unused	-

Table 5. Spearman correlation coefficients between predicted values and variables. †Indicates that the correlation is not significant ($p < 0.05$).

Variable	**Spearman CC 2001**	**Spearman CC 2009**	**Spearman CC 2016**
ELV	0.009†	-0.042†	-0.156
SLOPE	-0.528	-0.482	-0.334
TMI	0.372	0.236	0.096
WATER	-0.171	-0.074	-0.148
ROADS	-0.247	-0.281	-
REFOR	-0.294	-0.330	0.128
RESEV	-0.193	-0.295	-0.477
URBAN	-0.017†	-0.290	-0.189

4. Discussion

The implications of the results within the context of the disease management and the methodology applied are analyzed to further inform forest managers, farmers, and researchers, interested in preventing and reducing the incidence of oak decline in *dehesa* ecosystems.

4.1. Identification of affected and healthy spots

Frequently, remote sensing methods based on more or less automatic algorithms are used to monitor the occurrence of tree decline status in forests (Joshi et al., 2004; Kelly and Meentemeyer, 2002; Liu et al, 2006; Liu et al., 2007; Wilson et al., 2012). Nevertheless, the large scale of the study area (35,356 ha) and the highly variable range of symptoms the disease manifests, from sudden death to slow decline(Gallego et al., 1999; Moreira and Martins, 2005; de Sampaio e Paiva Camilo-Alves et al., 2013) makes difficult the direct application of traditional remote sensing methods to monitor occurrence of oak decline in this study(Liu et al., 2006). Moreover, Holmoak pruning,a common practice in *dehesa* management, could lead to misclassification of defoliated healthy trees (**Figure 2:C**). Visual interpretation of aerial imagery, although laborious, allowed the differentiation and suitable identification of affected trees and overcame some of the limitations of more automatic remote sensing approaches by enabling the identification of affected trees in heterogeneous scenarios. The limitations of traditional remote sensing methods for the detection of affected trees could be addressed with the development of methodologies based on high resolution imagery and machine learning(Carreiras et al., 2006; Liu et al., 2006), but looking backwards in time to dates of less quality imagery availability prevents this approach.

The identification of representative samples of healthy spots at tree crown level applying an object-based classification was achievable due to the uniform characteristic of Holmoak trees in the dehesa system in a date when the studied disease was almost absent in the area. The tree-covered area thus obtained was successively modified to produce the healthy areas in each study date by subtracting from it the visual-identified affected spots. The tree-cover classification showed acceptable overall accuracy (77%). Similar values of overall accuracy (78%) were reported by Godinho et al.,(2016) estimating *dehesa* canopy densities using Forest Canopy Density (FCD) model and Landsat-5 TM multispectral data. The object-based classification represents a significant improvement of existing methods for healthy

trees identification. Specifically, regarding the work presented in Abellanas et al., (2017), where random points generated in the whole study area represented healthy spots instead of allocating them in classified healthy tree-covered areas. This approach has allowed us to develop a presence-absence model considering true absences.

4.2.Spatial patterns of affected spots

The density maps derived from the visual identification of affected spots are consistent with the typical distribution of affected trees by *Phytophthora cinnamomi* in large groups of foci (Braisier, 1996). The aggregation of *Phytophthora*spp.foci following the appearance of the initial foci is well accepted in the literature and, together with the dependency between affected spots from different years shown by the bivariate cluster analysis, could indicate an epidemiological process (Kelly and Meentemeyer, 2002; D. Liu et al., 2007; Abellanas et al., 2017). This aligns with the hypothesis of *Phytophthora cinnamomi* being the main cause of oak decline in Mediterranean forests (Brasier et al., 1993; Brasier, 1996; Gallego et al., 1999; Sánchez et al., 2002; Sánchez et al., 2003; Moreira and Martins, 2005; de Sampaio e Paiva Camilo-Alves et al., 2013; Linaldeddu et al., 2014).

Results from the univariate cluster analysis for the three years were consistent in the clustering distance of affected spots (1,750 m). This has important implications for disease management as it could determine the size of surveillance and emergency areas around initial foci to be established to avoid disease spread. It also informs on the spatial scale in oak decline; studies at smaller scales may not be able to capture patterns occurring at landscape scale (Kelly and Meentemeyer, 2002).

The decrease of the peak clustering value over the years (**Figure4**) could indicate that the disease is changing to a different stage of spreading, colonizing new areas driven by vectors and factors less related to the initial foci. Results from the bivariate cluster analysis also indicate that affected spots could maintain their potential as a source of propagation of *Phytophthora cinnamomi* in long periods of time given that affected spots from 2016 still show a strong dependency of those infected in 2001 or before. The prevalence of *Phytophthora cinnamomi* in soil over the time has been pointed out in many studies (de Sampaio e Paiva Camilo-Alves et al., 2013; Hardham and Blackman, 2018; Sena et al., 2018).

4.3. Performance of MARS and landscape descriptors influence on the proneness to oak decline

Overall, the MARS models showed a strong relationship between the landscape descriptors selected and the presence/absence of infection. The decrease in the AUC values of MARS over time could be related to the increase of newly affected trees in successive dates, that has derived in an unbalanced prevalence in the successive models, as the area for the absences has simultaneously decreased (Raes and der Steege, 2007).

A total of eight out of ten landscape descriptors showed to be significant in the occurrence of oak decline, presenting remarkable changes in importance over the years. For all the models fitted, FLOWAC did not figure as a significant landscape descriptor and was excluded from the analysis. This could be due to the method used to extract flow accumulation values from the available DEM which may not be representative at the resolution and extent applied. Indexes such as TMI might capture the characteristics of the landscape in a better and more realistic way (Moore et al., 1991; Parker, 2013). The flow accumulation at 5m-grid resolution could represent values too local and variable, as its CV indicates (**Table 2**), to characterize processes occurring at landscape level.

The exclusion of ASPEC from all the models fitted disagreed with previous studies that found a higher occurrence of *Phytophthora cinnamomi* in southerly oriented slopes (Brasier, 1996; Moreira and Martins, 2005). This could be explained by the spatial configuration and extent of the study area; in an area dominated by rolling hills, other variables such as the geomorphology (valleys, hills, etc.) could outweigh the aspect effect on the moisture content of the locations considered by other authors.

The importance of SLOPE remains the highest every year, indicating a high explanatory value of this variable regarding the occurrence of oak decline. This agrees with Duque-Lazo et al., (2018) who found a negative correlation between slope and probability of occurrence of oak decline caused by *Phytophthora cinnamomi*. The authors related this to water carrying spores of *Phytophthora cinnamomi* being more easily stored in gentle slopes, while steeper slopes ease the drainage. It might be also related to erosion processes in steep slopes and sedimentation carrying spores in gentle slopes. In connection with that, Cardillo et al. (2018) demonstrated the development of *Phytophthora cinnamomi* patches downslope in Spanish heathlands.

The influence of soil moisture at landscape level has also been pointed out in many studies as a factor contributing to the proneness of infection by *Phytophthora cinnamomi* (Moreira and Martins, 2005; Vannini et al., 2010; Sena et al., 2018),and could also explain the importance of TMI and WATER in all the MARS models. The relationship between affected spots by *Phytophthora cinnamomi* occurrence and distance to watercourses is in

agreement with results from previous studies (Jules et al., 2002; Cardillo et al., 2012; Duque-Lazo et al., 2018). Similarly, for ELV the results obtained align with Wilson et al., (2003) and Václavík et al., (2010). In these studies, a significant negative correlation of elevation with the presence of *Phytophthora cinnamomi*wasreported. This could be explained by lower locations being more likely to receive spores carried by downhill water transport(Wilson et al., 2003).

Slope is also an important variable determining the intensity of management and impacts in *dehesa* ecosystems. Since topography is recognized to be a determining factor on the intensity of use (Herguido et al., 2017a; Veldkamp and Lambin, 2001), steeper slopes are expected to present less impact related to livestock, and agricultural activities such as plowing. Steeper areas are therefore less exposed to potential vectors of *Phytophthora cinnamomi* such as vehicles, animal hooves, workers' boots, etc. (Cardillo et al., 2018). Herguido et al., (2017b) also found slope as the most explanatory variable to model tree loss vs recruitment in *dehesas* using MARS, arguing that steeper slopes presented more tree recruitment due to the less intense management.

Of special relevance is the RI of REFOR in 2001 and 2009. As part of the afforestation subsidy program **1992 EEC Regulation 2080/92** promoted by the European Commission in 1992 to encourage the afforestation of agricultural lands (EU, 1992), 61,268 ha were afforested between 1994 and 2006 (especially in the first years) in Huelva province (Spain) with mainly Holm oak (*Quercus ilex*) and Cork oak (*Quercus suber*) (Jiménez and Navarro, 2014). The afforestation period coincides with the exponential spread of *Phytophthora cinnamomi* in this area (Abellanas et al., 2017). The infestation of nurseries with *Phytophthora spp.* in Europe has been proved in previous research studies (Brasier and Jung, 2003; Moralejo et al., 2009; Pérez-Sierra et al., 2013; Jung et al., 2016). It is therefore quite likely that the afforestation program relied, at least partly, on the use of infested nursery stock. This could have been one of the key vectors for the development of the foci/focus of *Phytophthora cinnamomi* within the study area. Similarly, a recent paper about "*Phytophthora infestations in European nurseries"* by Jung et al., 2016 reported the following results: "*90% of the containers stands of 11 oak species analyzed were infested with 16 Phytophthora species"* and "*Phytophthora cinnamomi was isolated in 18 of 21 Mediterranean oak plantings in Italy, Spain and Portugal*". From these results, they concluded, *"86% of these afforestations probably are infested by Phytophthora cinnamomi"* (Jung et al., 2016).

The research studies cited above are consistent with the results obtained for REFOR in our study; REFOR was the second most explanatory variable in 2001 and 2009, which

were the two periods where afforestations could act as the initial source of infection. In 2016, when the disease is widespread over the study area and the spread is less linked to the initial foci and driven by different factors, REFOR is the variable with the lowest RI. The fact that affected spots from 2001 and 2009 are not included in the data to fit the MARS model from 2016 could also affect the low RI of REFOR as most of the trees close to afforestations, the initial source of *Phytophthora cinnamomi,* could have died. This is confirmed by the positive Spearman correlation coefficient for REFOR in 2016 (**Table 5**), which indicates that unlike in 2001 and 2009, affected spots tend to be further away than healthy spots, due to the disappearance of the closest affected spots to afforestations from previous years.

The results here reported also showed that human factors could have an important role in the dynamics of oak decline at landscape level. URBAN maintained a high RI over time that suggests the highest occurrence of oak decline close to urban areas and artificial infrastructures. The association between *Phytophthora*spp.without aerial dispersal(Peterson et al., 2013; Peterson et al., 2014)and roads is well acknowledged by multiple authors (Brasier, 1996; Jules et al., 2002; Cardillo et al., 2012; Abellanas et al., 2017). For ROADS, the MARS model found the descriptor of importance for 2001 and 2009. ROADS was included in models from 2001 and 2009 and URBAN in all the three dates' models. This behavior aligns with the hypothesis of the influence of the human factor as a vector of *Phytophthora cinnamomi* at long distances. The contribution of human activity such as recreation and tourism to *Phytophthora cinnamomi* spread has been suggested in previous research (Pickering and Hill, 2007; Pickering et al., 2010; Rankin et al., 2015). Abellanas et al., (2017) also found a spatial relationship between oak decline spots and roads. Although in the present study WATER was included in the MARS model of 2009, this variable showed less importance (39,7%) than ROADS (52,8%) describing the distribution of affected spots. The exclusion of ROADS in 2016 could be explained by the predominance of the contagion process between trees over the transport of *Phytophthora cinnamomi* by roads or watercourses as the cause of new infections in 2016, when the disease is widespread along the study area.

Finally, the influence of RESEV seems to be linked to the use of reservoirs as drinking troughs for livestock, where the presence of livestock is more frequent and consequently the accumulation of spores carried by animal hooves to these areas is more likely. Brasier(1996) already mentioned the relation of oak decline with areas of heavy animal trampling, although it could be a combined effect with soil compaction which has also been demonstrated to have a strong association with oak decline (de Sampaio e Paiva Camilo-Alves et al., 2013). The increase of RI from 2001 to 2016 could be due to the consolidation of

a process pointing to mature stages of the disease rather than a primary process of the spread.

Although most of the landscape descriptors included in the analysis showed easy interpretation, meaningful RI and agreement with the literature, the importance of variables in MARS models has to be interpreted carefully since the dependent and independent variables do not necessarily follow a causal relationship (Herguido et al., 2017a). In addition, there are variables that are difficult to represent spatially at landscape level such as those related to the management, which have not been included in this study but could play an important role in the dynamics of oak decline. Studies following the same approach at farm level could further inform the spatio-temporal dynamics of oak decline in *dehesa* ecosystems. These studies might incorporate variables related to the management to further understand within-farm drivers of the disease and the differences in the dynamics at a broader scale investigated in this study.

5. Conclusion

It has been proved that oak decline has progressed significantly in the last two decades in “El Andevalo” region threatening the future of its *dehesas.* The studied patterns agree with the hypothesis of *Phytophthora cinnamomi* being the main cause of oak decline process in this area. Concerning the method, inhomogeneous Ripley's K-function allowed capturing spatial patterns, overcoming the limitation of the lack of stationarity. MARS demonstrated satisfactory performance dealing with a wide range of variables and reported meaningful and easily interpretable outcomes. Regarding the proposed objectives, the following conclusions are extracted:

i) Spatial pattern analysis with inhomogeneous Ripley's K-function allowed the identification of clustered patterns of affected spots in 1,750 m., showing a decrease of clustering overtime. The bivariate analysis demonstrated spatial dependency between affected spots from different years confirming the epidemic process.

ii) Variables directly and indirectly related to the soil moisture and water content at landscape level demonstrated to favor the presence of oak decline. The human factor and farm management seem to have an important role in the disease spreading. Afforestations conducted during the afforestation subsidy program of agricultural lands initiated in 1992 could have acted as the initial source of a massive *Phytophthora cinnamomi* infection.

The previous findings have important implications within the context of disease management. The scale of clustering (1,750m) could be taken as a reference to establish

areas of surveillance around initial foci, although the spreading at long distances needs to be also considered at the same time. The dependency between affected spots should be taken into account to prevent infection of *Phytophthora cinnamomi* to contiguous areas. From the point of view of preventive measures planning at landscape level, those locations that tend to store water should receive special attention. Managers should also consider the human factor and livestock habits when designing disease-managing planning given its potential to act as long-distance vectors. Afforestation programs must be carefully designed, ensuring the use of clean nursery stocks to avoid devastating effects caused by the introduction of invasive pathogens in forestry and agroforestry ecosystems. The disease tends to evolve to different stages of maturity where primary factors of dispersion, responsible for initial clustering, loss importance over time. Since the importance of variables seems to vary with both; the stage of the disease and the scale of the analysis, the consideration of temporal and spatial scale is of key importance when studying and planning oak decline management.

Acknowledgments

The authors would like to thank the Spanish Ministry of Economy and Competitiveness for funding the study (MINECO-INIA, project RTA2014-00063-C04-03).

Authors also would like to thank three anonymous reviewers for providing insightful suggestions that have allowed to significantly improve the paper.

This study is part of a master thesis submitted at Cranfield University to complete the degree of MSc in Geographical Information Management.

References

Abellanas, B., Fernández Rebollo, P., Hidalgo Fernández, M.T., Leal Murillo, J. R., Carbonero Muñoz M.D., Gonzalez Dugo, M., 2017. Análisis espacial de la evolución del decaimiento de Quercus: relación con las estructuras lineales del paisaje. *7º Congreso Forestal Español*,pp.1-14.26-30 June, Plasencia,Spain.

Baddeley, A., 2010. *Analysing spatial point patterns in R.* Technical Report.CSIRO and University of Western Australia, Version 4, 1–232. https://doi.org/10.1007/s00415-011-6369-2

Baddeley, A., Diggle, P. J., Hardegen, A., Lawrence, T., Milne, K.,& Nair, G., 2014. On tests of spatial pattern based on simulation envelopes. *Ecol. Monogr., 84*, 477–489.https://doi.org/10.1890/13-2042.1

Baddeley, A., Moller, J., & Waagepetersen, R., 2000. Non- and semi-parametric estimation of interaction in inhomogeneous point patterns. *Stat. Neerl.*, *54*, 329–350. https://doi.org/10.1111/1467-9574.00144

Baddeley, A., Turner, R., & Runbak, E., 2018. Package "spatstat"*1.56-1*.Technical Report. Available at: http://spatstat.org/releasenotes/spatstat-1.56-1.html; last accessed July 2018.

Bergot, M., Cloppet, E., Perarnaud,V.,Déqué, M., Marçais, B., Desprez-Loustau, M.L., 2004. Simulation of potential range expansion of oak disease caused by *Phytophthora cinnamomi* under climate change. *Glob. Change Biol.*, *10*, 1539–1552. https://doi.org/10.1111/j.1365-2486.2004.00824.x

Besag, J. E., 1977. Discussion contribution to Ripley (1977). *J. R. Stat. Soc.*, *39*, 193–195.

Brasier, C. M., 1996. *Phytophthora cinnamomi* and oak decline in southern Europe. Environmental constraints including climate change. *Ann. Sci. Forest.*, *53*, 347–358. https://doi.org/10.1051/forest:19960217

Brasier, C.M., Robredo, F.; Ferraz, J. F. P., 1993. Evidence for *Phytophthora cinnamomi* involvement in Iberian oak decline. *Plant Pathol.*, *42*, 140–145. https://doi.org/10.1111/j.1365-3059.1993.tb01482.x

Brasier, C. M., Jung, T., 2003. Progress in understanding Phytophthora diseases of trees in Europe. In: *Phytophthora* in forests and natural ecosystems. Proc. 2nd Int. *IUFRO Working Party 7.02.09 Meeting*, Albany, Western Australia. September 30–October 5, 2001. Ed. by McComb, J. A.; Hardy, G. E. StJ. Perth: Murdoch University Print, pp. 4–18.

Brodie, C., Houle, G., Fortin, M.J., 1995. Development of a *Populus balsamifera* Clone in Subarctic Quebec Reconstructed from Spatial Analyses. *J. Ecol.*, *83*, 309–320. https://doi.org/10.2307/2261569

Bugalho, M. N., Caldeira, M. C., Pereira, J. S., Aronson, J., Pausas, J. G.,2011. Mediterranean Cork oak savannas require human use to sustain biodiversity and ecosystem services. *Front. Ecol. Environ.*, 9, 278-286.https://doi.org/10.1890/100084

Burgess, T. I., Scott, J. K., Mcdougall, K. L., Stukely, M. J. C., Crane, C., Dunstan, W. A., Brigg, F.,Andjic, V., White, D., Rudman, T., Arentz, F., Ota, N., Hardy, G. E. S. J., 2017. Current and projected global distribution of *Phytophthora cinnamomi*, one of the world's

worst plant pathogens. *Glob. Change Biol.*, *23*, 1661–1674. https://doi.org/10.1111/gcb.13492

Burrough, P. A., McDonell, R. A.,1998. *Principles of Geographical Information Systems*. O. U. Press, Ed. New York.

Cahill, D. M., Rookes, J. E., Wilson, B. A., Gibson, L., McDougall, K. L.,2008.*Phytophthora cinnamomi* and Australia's biodiversity: Impacts, predictions and progress towards control. *Aust. J. Bot.*, *56*, 279–310. https://doi.org/10.1071/BT07159

Cardillo, E., Acedo, A., Abad, E., 2018. Topographic effects on dispersal patterns of *Phytophthora cinnamomi* at a stand scale in a Spanish heathland. *PloS one*, 13, 2-30. https://doi.org/10.1371/journal.pone.0195060

Cardillo, E.; Acedo, A., Perez ,C.,2012. Spatial patterns of Holm oak decline in Extremadura, Spain. In:*6th IUFRO Working Party 7.02.09 "Phytophthora in Forests and Natural Ecosystems".*9-12 September, Cordoba, Spain.

Carrasco, A., 2009. *Procesos de decaimiento forestal (la Seca):situación del conocimiento.*Consejería de Medio Ambiente, Junta de Andalucía, Córdoba.

Carreiras, J. M. B., Pereira, J. M. C., Pereira, J. S., 2006. Estimation of tree canopy cover in evergreen oak woodlands using remote sensing. *Forest Ecol. Manag.*, *223*, 45–53. https://doi.org/10.1016/j.foreco.2005.10.056

Costa, A., Pereira, H., Madeira, M., 2010. Analysis of spatial patterns of oak decline in Cork oak woodlands in Mediterranean conditions. *Ann. Forest Sci.,* 67, 204. https://doi.org/10.1051/forest/2009097

Costa, J. C., Martín, A., Fernández, R., Estirado, M., 2006. *Dehesas de Andalucía: caracterización ambiental*. Consejería de Medio Ambiente de la Junta de Andalucía.

Craven, P., Wahba, G., 1978. Smoothing noisy data with spline functions. *Numer. Math.*, *31*, 377–403.https://rdcu.be/8tMU; last accessed August 2018.

de Sampaio e Paiva Camilo-Alves, C., da Clara, M. I. E., de Almeida Ribeiro, N. M. C., 2013. Decline of Mediterranean oak trees and its association with *Phytophthora cinnamomi*: A review. *Eur. J. Forest Res.*, *132*,411-432.

De Veaux, R. D., Psichogios, D. C., Ungar, L. H.,1993. A comparison of two nonparametric estimation schemes: MARS and neural networks. *Comput. Chem. Eng., 17*, 819-

837.https://doi.org/10.1016/0098-1354(93)80066-V

DeLeo, J. M., 1993. Receiver operating characteristic laboratory (ROCLAB): software for developing decision strategies that account for uncertainty. In: *Uncertainty Modeling and Analysis, 1993. Proceedings., Second International Symposium*(April) (pp. 318-325). IEEE. https://doi.org/10.1109/ISUMA.1993.366750

Díaz, M., Pulido, F., Marañon, T., 2003. Diversidad biológica y sostenibilidad ecológica y económica de los sistemas adehesados. *Revista Ecosistemas*, *12*http://www.aeet.org/ecosistemas/033/investigacion4.htm

Dinis C. 2014. Cork oak (Quercus suber L.) root system: a structural-funtional 3D approach. PhD thesis. University of Evora, Portugal. pp 174.

Duque-Lazo, J., Navarro-Cerrillo, R. M., van Gils, H., Groen, T. A., 2018. Forecasting oak decline caused by *Phytophthora cinnamomi* in Andalusia: Identification of priority areas for intervention. *Forest Ecol. Manag.*, *417*, 122–136. https://doi.org/10.1016/j.foreco.2018.02.045

Duque-Lazo, J., van Gils, H., Groen, T. A., Navarro-Cerrillo, R. M., 2016. Transferability of species distribution models: The case of *Phytophthora cinnamomi* in Southwest Spain and Southwest Australia. *Ecol. Model.*, *320*, 62–70. https://doi.org/10.1016/j.ecolmodel.2015.09.019

Eccles, N. S., Esler, K. J., Cowling, R. M., 1999. Spatial pattern analysis in Namaqualand desert plant communities: evidence for general positive interactions. *Plant Ecol.*, *142*, 71–85. https://doi.org/10.1023/a:1009857824912

ESRI, 2016. ArcGIS Release 10.5. Redlands, CA. Retrieved from https://www.esri.com/arcgis-blog/products/apps/announcements/arcgis-10-5-new-release-transforms-enterprise-gis/; last accessed June 2018

EU, 1992. Council Regulation (EEC) No 2080/92 of 30 June 1992 Instituting a Comunity aid Scheme for Forestry Measures in Agriculture Fearnside. *Official Journal of European Communities*, (2080), 96–99. Available at: https://publications.europa.eu/en/publication-detail/-/publication/c9fb7e00-b01b-4d9a-8e58-54ca5ac61cbb/language-en

Fernández-Rebollo, P., García, A., Abellanas, B., Mata, R., Gómez, J.L., Leal, J.R., 2017. Assessing Oak replacement in dehesa system through in-plot analysis. Integrated Protection in oak Forests IOBC-WPRS Bulletin Vol. 127: 170-177.

Fibich, P., Lepš, J., Novotný, V., Klimeš, P., Těšitel, J., Molem, K., Damas, K., Weiblen, G. D., 2016. Spatial patterns of tree species distribution in New Guinea primary and secondary lowland rain forest. *J. Veg. Sci.*, *27*, 328–339. https://doi.org/10.1111/jvs.12363

Fielding, A. H., Bell, J. F., 1997. A review of methods for the assessment of prediction errors in conservation presence / absence models. *Environ. Conserv.*, *24*, 38–49. https://doi.org/10.1017/S0376892997000088

Friedman, J. H.,1991. Multivariate adaptive regression splines. *Ann. Stat.*, *9*, 1–67. Retrieved from https://www.jstor.org/stable/2241837

Gallego, F. J., Perez De Algaba, A., Fernandez-Escobar, R.,1999. Etiology of oak decline in Spain. *Eur. J. Forest Pathol.*, *29*, 17–27. https://doi.org/10.1046/j.1439-0329.1999.00128.x

Getzin, S., Wiegand, T., Wiegand, K., He, F., 2008. Heterogeneity influences spatial patterns and demographics in forest stands. *J. Ecol.*, *96*, 807–820. https://doi.org/10.1111/j.1365-2745.2007.0

Godinho, S., Gil, A., Guiomar, N., Neves, N., Pinto-Correia, T., 2016. A remote sensing-based approach to estimating montado canopy density using the FCD model: a contribution to identifying HNV farmlands in southern Portugal. *Agroforest. Syst.*, *90*, 23–34. https://doi.org/10.1007/s10457-014-9769-3

Gómez Gutiérrez, Á., Schnabel, S., Felicísimo, A. M., 2009a. Modelling the occurrence of gullies in rangelands of southwest Spain. *Earth Surf. Proc. Land.*, *34*, 1894–1902. https://doi.org/10.1002/esp.1881

Gómez Gutiérrez, Á. G., Schnabel, S., Lavado Contador, J. F., 2009b. Using and comparing two nonparametric methods (CART and MARS) to model the potential distribution of gullies. *Ecol. Model.*, *220*, 3630–3637. https://doi.org/10.1016/j.ecolmodel.2009.06.020

Haase, P.,1995. Spatial pattern analysis in ecology based on Ripley's K-function: Introduction and methods of edge correction. *J. Veg. Sci.*, *6*, 575–582. https://doi.org/10.2307/3236356

Hardham, A. R., Blackman, L. M., 2018. *Phytophthora cinnamomi*. *Mol. Plant Pathol.*, *19*, 260–285. https://doi.org/10.1111/mpp.12568

Herguido, E., Lavado Contador, J. F., Gómez Gutiérrez, Á., Schnabel, S., 2017a. Modeling

Tree Loss Versus Tree Recruitment Processes in SW Iberian Rangelands as Influenced by Topography and Land use and Management. *Land Degrad. Dev.*, *28*, 1652–1664. https://doi.org/10.1002/ldr.2697

Herguido, E., Lavado Contador, J. F., Pulido, M., Schnabel, S., 2017b. Spatial patterns of lost and remaining trees in the Iberian wooded rangelands. *Appl. Geogr.*, *87*, 170–183. https://doi.org/10.1016/j.apgeog.2017.08.011

Holdenrieder, O., Pautasso, M., Weisberg, P. J., Lonsdale, D., 2004. Tree diseases and landscape processes: The challenge of landscape pathology. *Trends Ecol. Evol.*, *19*, 446–452. https://doi.org/10.1016/j.tree.2004.06.003

IGN, 2018. Instituto Geográfico Nacional.Available at: http://www.ign.es/web/ign/portal; last accessed August 2018

Jenson, S. K., Domingue, J. O., 1988. Extracting topographic structure from digital elevation data for geographic information system analysis. *Photogramm. Eng. Rem. S.*, *54*, 1593–1600. https://doi.org/0099-1112/88/5411-1593$02.25/0

Jiménez, M. N., Navarro, F., 2014. *Programa de forestación de tierras agrarias en Andalucía: legislación y situación actual*. Junta de Andalucía. Instituto de Investigación y Formación Agraria y Pesquera. Consejería de Agricultura, Pesca y Desarrollo Rural.Granada, Julio de 2014.Available at: https://docplayer.es/78478967-Programa-de-forestacion-de-tierras-agrarias-en-andalucia-legislacion-y-situacion-actual.html; last accessed July 2018

Joshi, C., De Leeuw, J.,van Duren, I.C., 2004. Remote sensing and GIS applications for mapping and spatial modelling of invasive species.*Proceedings of ISPRS vol. 35*, B7 (7), Istanbul, pp. 669–77.

Jules, E. S., Kauffman, M. J., Ritts, W. D., Carroll, A. L., 2002. Spread of an invasive pathogen over a variable landscape: a nonnative root rot on Port Orford cedar. *Ecology*, 83, 3167-3181..https://doi.org/10.1890/0012-9658(2002)083[3167:SOAIPO]2.0.CO;2

Jung, T., Blaschke, H., Oßwald, W., 2000. Involvement of soilborne Phytophthora species in Central European oak decline and the effect of site factors on the disease. *Plant Pathol.*, 49, 706-718.

Jung, T., Chang, T. T., Bakonyi, J., Seress, D., Pérez-Sierra, A., Yang, X., Hong, C., Scanu, B., Fu, C.H., Hsueh, K.L., Maia, C., Abad-Campos, P., León, M., Horta Jung, M., 2017.

Diversity of Phytophthora species in natural ecosystems of Taiwan and association with disease symptoms. *Plant Pathol.*, 66, 194–211. https://doi.org/10.1111/ppa.12564

Jung, T., Colquhoun, I. J., Hardy, G. S. J.,2013. New insights into the survival strategy of the invasive soilborne pathogen Phytophthora cinnamomi in different natural ecosystems in Western Australia. *Forest Pathol.*, 43, 266-288.

Jung, T., Orlikowski, L., Henricot, B., Abad-Campos, P., Aday, A. G., Aguín Casal, O., Bakonyi,J., Cacciola,S. O., Cech,T., Chavarriaga,D., Corcobado,T., Cravador,A., Decourcelle,T., Denton,G., Diamandis,S., Doğmuş- Lehtijärvi,H. T., Franceschini,A., Ginetti,B., Green,S.,Glavendekić,M., Hantula,J., Hartmann,G., Herrero,M., Ivic,D., Horta Jung,M., Lilja,A., Keca,N., Kramarets,V., Lyubenova,A., Machado,H., Magnano di San Lio,G., Mansilla Vázquez,P. J., Marçais,B., Matsiakh,I., Milenkovic,I., Moricca,S., Nagy,Z. Á., Nechwatal,J., Olsson,C., Oszako,T., Pane,A., Paplomatas, E. J. Pintos Varela,C., Prospero,S., Rial Martínez,C., Rigling,D., Robin,C., Rytkönen,A., Sánchez,M. E., Sanz Ros,A. V., Scanu,B., Schlenzig,A., Schumacher,J., Slavov,S., Solla,A., Sousa,E., Stenlid,J., Talgø,V., Tomic,Z., Tsopelas,P., Vannini,A., Vettraino,A. M., Wenneker,M., Woodward,S., Peréz-Sierra, A., 2016. Widespread Phytophthora infestations in European nurseries put forest, semi-natural and horticultural ecosystems at high risk of Phytophthora diseases. *Forest Pathol.*, *46*, 134–163. https://doi.org/10.1111/efp.12239

Jung, T., Pérez-Sierra, A., Durán, A., Horta, M. J., Balci, Y., Scanu, B., 2018. Canker and decline diseases caused by soil-and airborne Phytophthora species in forests and woodlands. *Persoonia: Molecular Phylogeny and Evolution of Fungi*, 40, 182-220.

Kelly, M., Meentemeyer, R. K., 2002,. Landscape dynamics of the spread of sudden oak death. *Photogramm. Eng. Rem. S.*, *68*, 1001–1009.

Leathwick, J. R., Rowe, D., Richardson, J., Elith, J., Hastie, T., 2005. Using multivariate adaptive regression splines to predict the distributions of New Zealand's freshwater diadromous fish. *Freshwater Biol.*, *50*, 2034–2052. https://doi.org/10.1111/j.1365-2427.2005.01448.x

Lin, Y. C., Chang, L. W., Yang, K. C., Wang, H. H., Sun, I. F., 2011. Point patterns of tree distribution determined by habitat heterogeneity and dispersal limitation. *Oecologia*, *165*(1), 175–184. https://doi.org/10.1007/s00442-010-1718-x

Linaldeddu, B. T., Scanu, B., Maddau, L., Franceschini, A., 2014. Diplodia corticola and

Phytophthora cinnamomi: the main pathogens involved in Holm oak decline on C aprera I sland (I taly). *Forest Pathol.*, 44, 191-200.

Linea., 2018. Localizador de Información Espacial de Andalucía.Available at:http://www.juntadeandalucia.es/institutodeestadisticaycartografia/lineav2/web/

Liu, D., Kelly, M., Gong, P., 2006. A spatio-temporal approach to monitoring forest disease spread using multi-temporal high spatial resolution imagery. *Remote Sens. Environ.*, *101*, 167–180. https://doi.org/10.1016/j.rse.2005.12.012

Liu, D., Kelly, M., Gong, P., Guo, Q., 2007. Characterizing spatio-temporal tree mortality patterns associated with a new forest disease. *Forest Ecol. Manag.*, *253*, 220–231. https://doi.org/10.1016/j.foreco.2007.07.020

Liu, Y., Li, F., Jin, G., 2014. Spatial patterns and associations of four species in an old-growth temperate forest. *J. Plant Interact.*, *9*, 745–753. https://doi.org/10.1080/17429145.2014.925146

Loosmore, N. B., Ford, E. D., 2006. Statistical Inference Using The G Or K Point Pattern Spatial Statistics. *Ecology*, *87*, 1925–1931. https://doi.org/10.1890/0012

Luque, G. M., Bellard, C., Bertelsmeier, C., Bonnaud, E., Genovesi, P., Simberloff, D., Courchamp, F., 2014. The 100th of the world's worst invasive alien species. *Biol.Invasions*, *16*, 981–985. https://doi.org/10.1007/s10530-013-0561-5

Martín, D., Campos, P., Cañellas, I., Montero, G., 2001. Extended cost benefit analysis of Holm oak dehesa multiple use and cereal grass rotations. *Invest. Agrar-Sist. Rec. F.*, *10*, 109–124.

Meyer, S., Held,L., Höhle, M., 2017. Spatio-Temporal Analysis of Epidemic Phenomena Using the R Package surveillance. *J. Stat.Softw.,77doi:10.18637/jss.v077.i11*

Milborrow, S., 2018a. Notes on the earth package. Technical report, 1–60. Available at: http://www.milbo.org/doc/earth-notes.pdf; last accessed July 2018

Milborrow, S., 2018b. *Package "Earth"*. Technical Report.Available at: https://cran.r-project.org/web/packages/earth/earth.pdf; last accessed July 2018

Moore, I. D., Grayson, R. B., Ladson, A. R., 1991. Digital terrain modelling: A review of hydrological, geomorphological, and biological applications. *Hydrol. Process.*, *5*, 3–30.https://doi.org/10.1002/hyp.3360050103

Moralejo, E., Pérez-Sierra, A. M., Álvarez, L. A., Belbahri, L., Lefort, F., Descals, E., 2009. Multiple alien Phytophthora taxa discovered on diseased ornamental plants in Spain. *Plant Pathol.*, *58*, 100–110. https://doi.org/10.1111/j.1365-3059.2008.01930.x

Moreira, A. C., Martins, J. M. S., 2005. Influence of site factors on the impact of *Phytophthora cinnamomi* in Cork oak stands in Portugal. *Forest Pathol.*, *35*, 145–162. https://doi.org/10.1111/j.1439-0329.2005.00397.x

Moreno, G., Pulido, F. J., 2009. *The functioning, management and persistence of dehesas.*In: Rigueiro-Rodríguez A, McAdam J, Mosquera-Losada MR (eds) Agroforestry in Europe, current status and future prospects, pp 127–160. Springer, Dordrecht.

Muñoz, J., Felicísimo, A. M., 2004. Comparison of statistical methods commonly used in predictive modelling. *Journal of Vegetation Science*, *15*, 285–292. https://doi.org/10.1658/1100-9233(2004)015[0285:COSMCU]2.0.CO;2

Myllymäki, M., Mrkvička, T., Grabarnik, P., Seijo, H., Hahn, U., 2017. Global envelope tests for spatial processes. *J. Roy. Stat. Soc.B*, *79*, 381–404. https://doi.org/10.1111/rssb.12172

Natalini, F., Alejano, R., Vázquez-Piqué, J., Cañellas, I., Gea-Izquierdo, G., 2016. The role of climate change in the widespread mortality of Holm oak in open woodlands of Southwestern Spain. *Dendrochronologia, 38*, 51-60.https://doi.org/10.1016/j.dendro.2016.03.003

Parker, A. J., 2013. The Topographic Relative Moisture Index: An Approach to Soil-Moisture Assessment in Mountain Terrain. *Phys. Geogr.*, *3*, 160–168. https://doi.org/10.1080/02723646.1982.10642224.

Pearce, J. L., Ferrier, S., 2000. Evaluating the predictive performance of habitat models developed using logistic regression. *Ecol. Model.*, *133*, 225–245. https://doi.org/10.1016/S0304-3800(00)00322-7

Pérez-Sierra, A., López-García, C., León, M., García-Jiménez, J., Abad-Campos, P., Jung, T., 2013. Previously unrecorded low-temperature Phytophthora species associated with Quercus decline in a Mediterranean forest in eastern Spain. *Forest Pathol.*, *43*, 331–339. https://doi.org/10.1111/efp.12037

Peterson, E., Hansen, E., Hulbert, J., 2014. Source or sink? The role of soil and water borne

inoculum in the dispersal of Phytophthora ramorum in Oregon tanoak forests. *Forest Ecol. Manag.*, *322*, 48–57. https://doi.org/10.1016/j.foreco.2014.02.031

Peterson, E., Hansen, E., Kanaskie, A., 2013. Spatial relationship between Phytophthora ramorum and roads or streams in Oregon tanoak forests. *Forest Ecol. Manag., 312*, 216–224. https://doi.org/10.1016/j.foreco.2013.10.002

Pickering, C. M., Hill, W., 2007. Impacts of recreation and tourism on plant biodiversity and vegetation in protected areas in Australia. *J. Environ. Manage., 85,* 791-800.https://doi.org/10.1016/j.jenvman.2006.11.021

Pickering, C. M., Hill, W., Newsome, D., Leung, Y. F., 2010. Comparing hiking, mountain biking and horse riding impacts on vegetation and soils in Australia and the United States of America. *J. Environ. Manage.,* 91, 551-562.https://doi.org/10.1016/j.jenvman.2009.09.025

Plieninger, T., Wilbrand, C., 2001. Land use, biodiversity conservation, and rural development in the dehesas of Cuatro Lugares, Spain. Agroforest. Syst., 51, 23-34.https://rdcu.be/8pGe

Ploetz, R. C., 2013. Phytophthora root rot of Avocado. In C. International (Ed.), *Phytophthora: A Global Perspective*, pp. 197–203. Wallingford, Oxfordshire.

Raes, N., der Steege, H., 2007. A null-model for significance testing of presence-only species distribution *models.Ecography, 30, 727-736.*https://doi.org/10.1111/j.2007.0906-7590.05041.x

Rankin, B. L., Ballantyne, M., Pickering, C. M., 2015. Tourism and recreation listed as a threat for a wide diversity of vascular plants: A continental scale review.*J. Environ. Manage., 154*, 293-298.https://doi.org/10.1016/j.jenvman.2014.10.035

REDIAM., 2018. Red de Información Ambiental de Andalucía. Consejería de Medio Ambiente y Ordenación del Territorio. Available at: http://www.juntadeandalucia.es/medioambiente/site/rediam; last accessed June 2018

Ripley, B. D., 1977. Modelling Spatial Patterns. *J. Roy. Stat. Soc. B*, *39*, 172–212. Retrieved from https://www.jstor.org/stable/2984796

Ripley, B. D., 1991. *Statistical inference for spatial processes*. Cambridge University press,New York, USA.

Ristaino, J. B., Gumpertz, M. L., 2000. New frontiers in the study of dispersal and spatial analysis of epidemics caused by species in the genus Phytophthora. *Annu. Rev. Phytopathol.*, *38*, 541–576. https://doi.org/0066-4286/00/0901-0541$14.00

Sánchez, M. E., Caetano, P., Ferraz, J., Trapero, A., 2002. Phytophtora disease of Quercus ilex in south-western Spain. *Forest Pathol.*, *32*, 5–18. https://doi.org/10.1046/j.1439-0329.2002.00261.x

Sánchez, M., Sánchez, J.E., Navarro-Cerrillo, R.M., Fernández-Rebollo, P., Trapero, A., 2003. Incidencia de la podredumbre radical causada por *Phytophthora cinnamomi* en masas de Quercus en Andalucía. *Boletín de Sanidad Vegetal y Plagas*, *29*, 87–108.

Sena, K., Crocker, E., Vinpixeli, P., Barton, C., 2018. *Phytophthora cinnamomi* as a driver of forest change: Implications for conservation and management. *Forest Ecol. Manag., 409*, 799–807. https://doi.org/10.1016/j.foreco.2017.12.022

Sharda, V. N., Prasher, S. O., Patel, R. M., Ojasvi, P. R., Prakash, C., 2008. Performance of Multivariate Adaptive Regression Splines (MARS) in predicting runoff in mid-Himalayan micro-watersheds with limited data. *Hydrolog. Sci. J., 53*, 1165-1175.https://doi.org/10.1623/hysj.53.6.1165

Swets, J. A., 1988. Measuring the accuracy of diagnostic systems. *Science, 240*, 1285-1293.

Szwagrzyk, J., Czerwczak, M., 1993. Spatial Patterns of Trees in Natural Forests of East-Central-Europe. *J. Veg. Sci.*, *4*, 469–476.https://doi.org/10.2307/3236074

Thomas, F. M., Blank, R., Hartmann, G., 2002. Abiotic and biotic factors and their interactions as causes of oak decline in Central Europe. *Forest Pathol.*, 32, 277-307.

Vacek, S., Lepš, J., 1996. Spatial dynamics of forest decline: the role of neighbouring trees. *J. Veg. Sci.*, *7*, 789–798. https://doi.org/10.2307/3236457

Václavík, T., Kanaskie, A., Goheen, E., Ohmann, J., Hansen, E., Meentemeyer, R., 2010. Mapping the Risk of Sudden Oak Death in Oregon : Prioritizing Locations for Early Detection and Eradication.General Technical Report PSW-GTR-229. *Fourth Sudden Oak Death Science Symposium*, 126–132. June 15-18, 2009, Santa Cruz, California

Vannini, A., Natili, G., Anselmi, N., Montaghi, A., Vettraino, A. M., 2010. Distribution and gradient analysis of Ink disease in chestnut forests. *Forest Pathol.*, *40*, 73–86. https://doi.org/10.1111/j.1439-0329.2009.00609.x

Velázquez, E., Martínez, I., Getzin, S., Moloney, K. A., Wiegand, T., 2016. An evaluation of the state of spatial point pattern analysis in ecology. *Ecography*, *39*, 1042–1055. https://doi.org/10.1111/ecog.01579

Veldkamp, A., Lambin, E. F., 2001. Predicting land-use change. *Agr. Ecosyst. Environ.*, *85*, 1–6. https://doi.org/10.1016/S0167-8809(01)00199-2

Wiegand, T., 2004. *Introduction to point pattern analysis with Ripley's L and the O-ring statistic using the Programita software.* (Vol. 2). Leipzig.

Wilson, B. A., Lewis, A., Aberton, J., 2003. Spatial model for predicting the presence of cinnamon fungus (*Phytophthora cinnamomi*) in sclerophyll vegetation communities in south-eastern Australia. *Austral Ecol.*, *28*, 108–115.

Wilson, B. A., Zdunic, K., Kinloch, J., Behn, G., 2012. Use of remote sensing to map occurrence and spread of *Phytophthora cinnamomi* in Banksia woodlands on the Gnangara Groundwater System, Western Australia. *Aust. J. Bot.*, *60*, 495–505. https://doi.org/10.1071/BT11305

Zentemeyer, G., 1980. *Phytophthora cinnamomi and the diseases it causes*. *MonographA.P.S. Symp.Ser*.(10th ed.). St. Paul, Minn.:

Figure (Supplementary Material)
Click here to download Figure: Figure_SM1.pdf

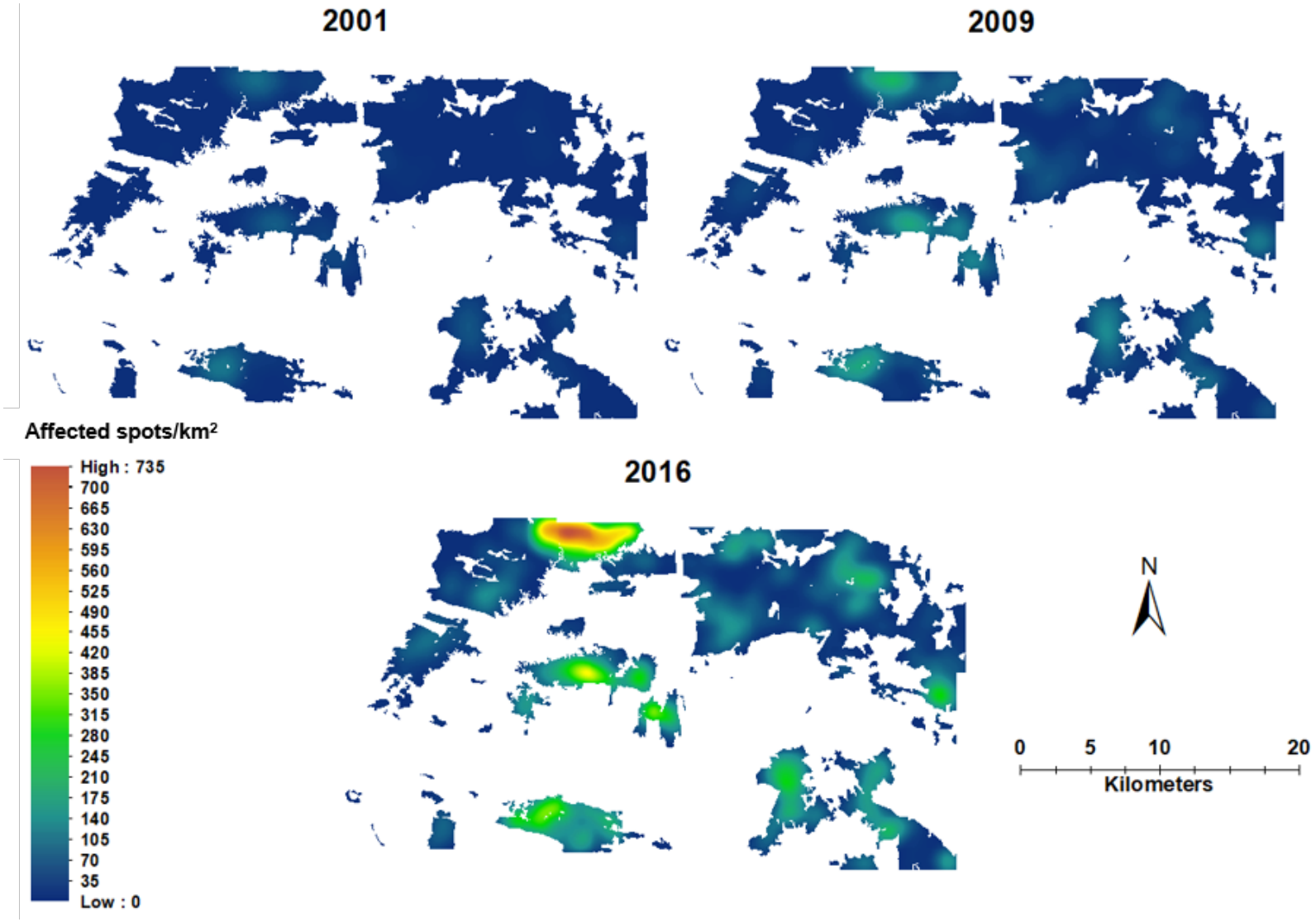

Figure SM_1. Kernel density maps of oak decline affected spots in 2001, 2009 and 2016. The affected spots of the consecutive years have been aggregated.

Figure (Supplementary Material)
Click here to download Figure: Figure_SM2.pdf

Figure SM_2.- Density functions of MARS model selected descriptors in affected (red) and healthy (blue) spots along the study years.

	2001	2009	2016
SLOPE	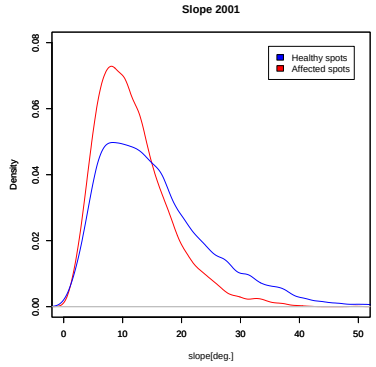	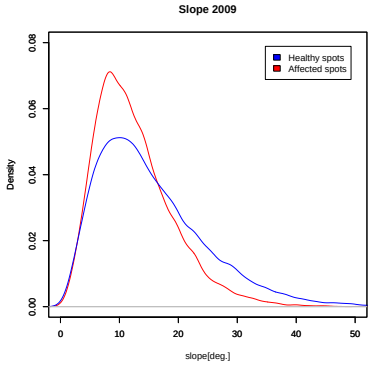	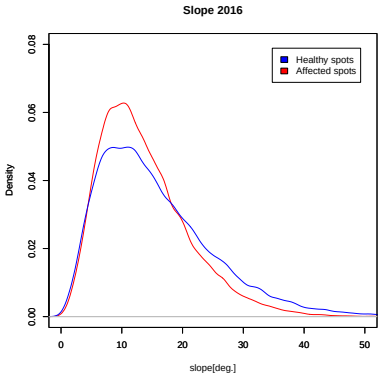
REFOR	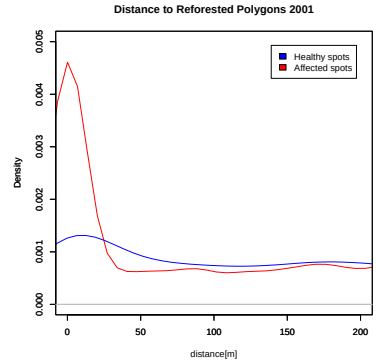	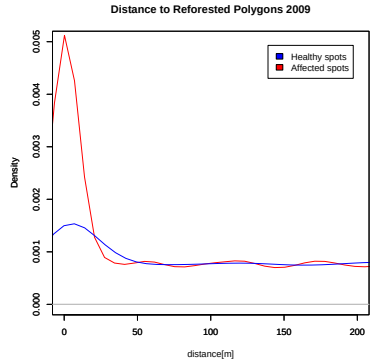	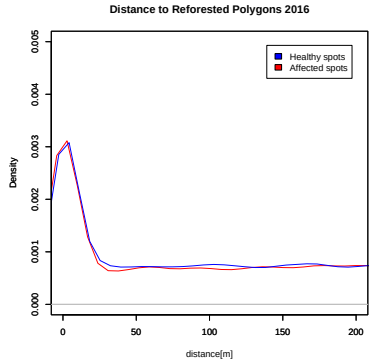
WATER	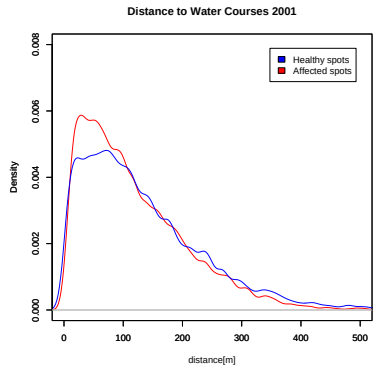	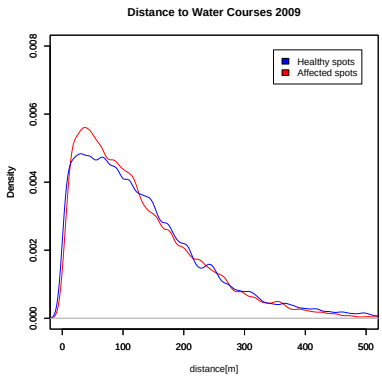	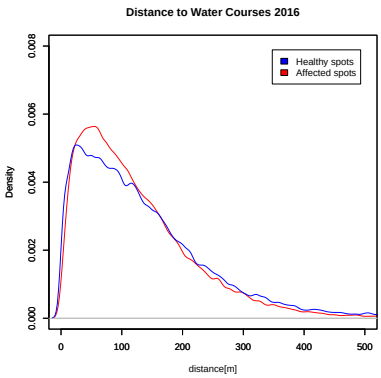
URBAN	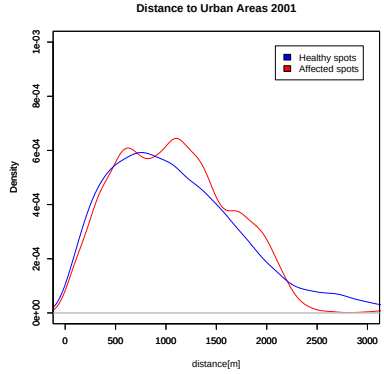	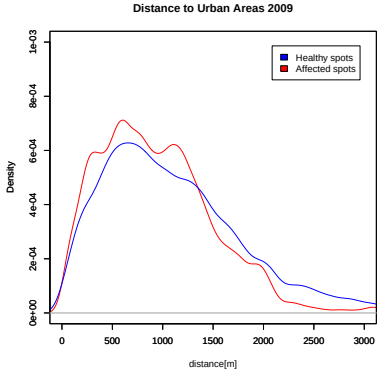	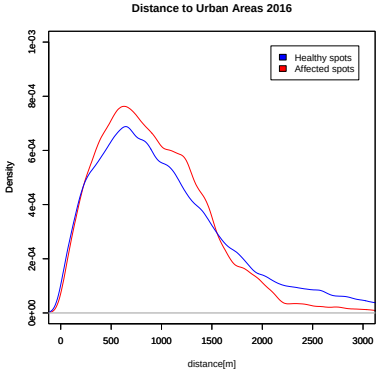

	2001	2009	2016
ELV	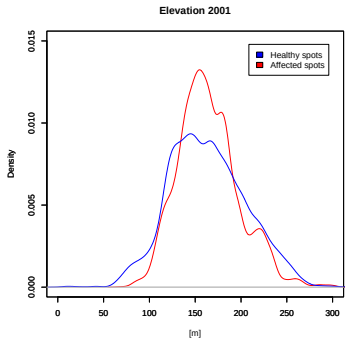	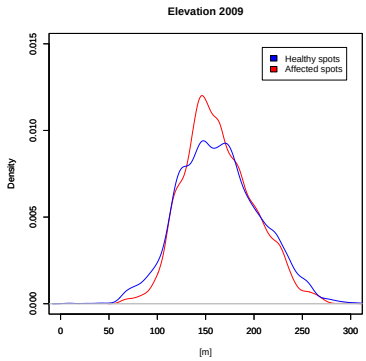	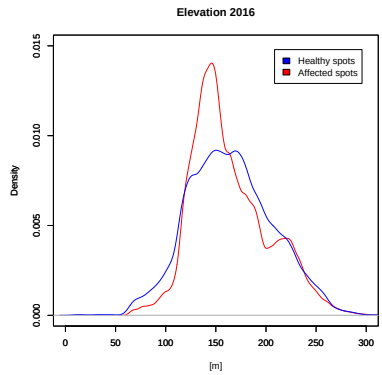
TMI	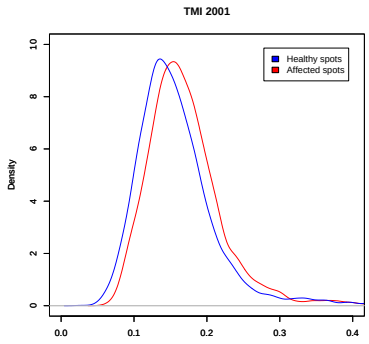	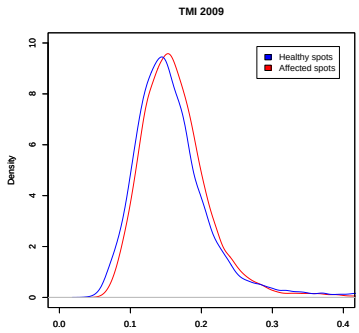	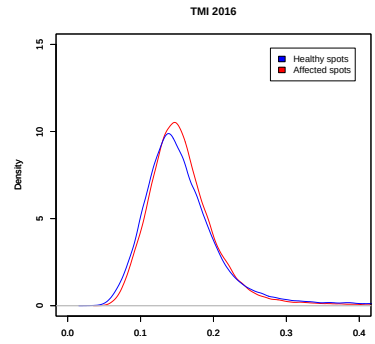
ROADS	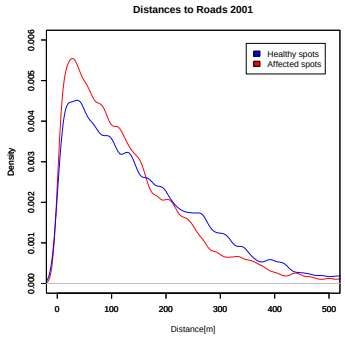	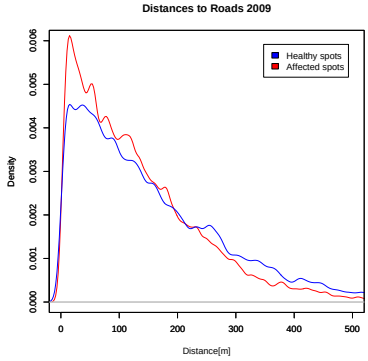	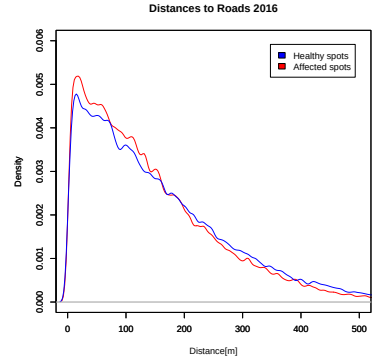
RESEV	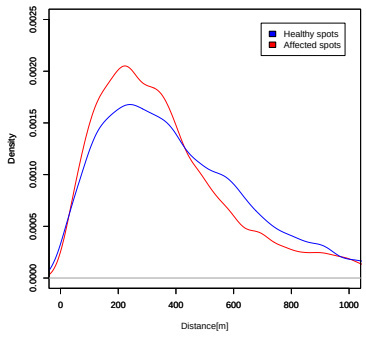	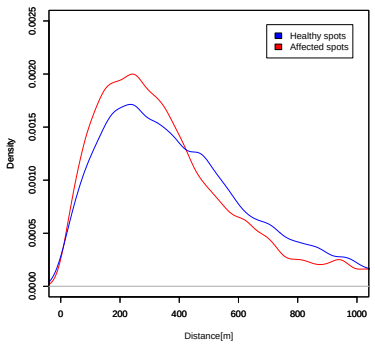	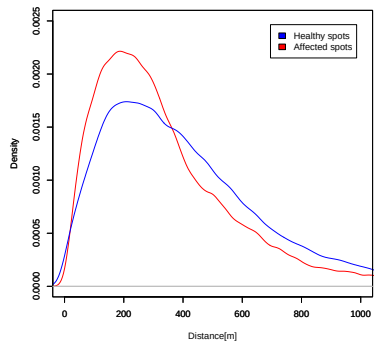

Figure(Supplementary Material)

Click here to download Figure: Figure SM3.docx.pdf

Figure SM3. Initial tree-covered area within the study area, obtained by an object-based clasification method (1998)

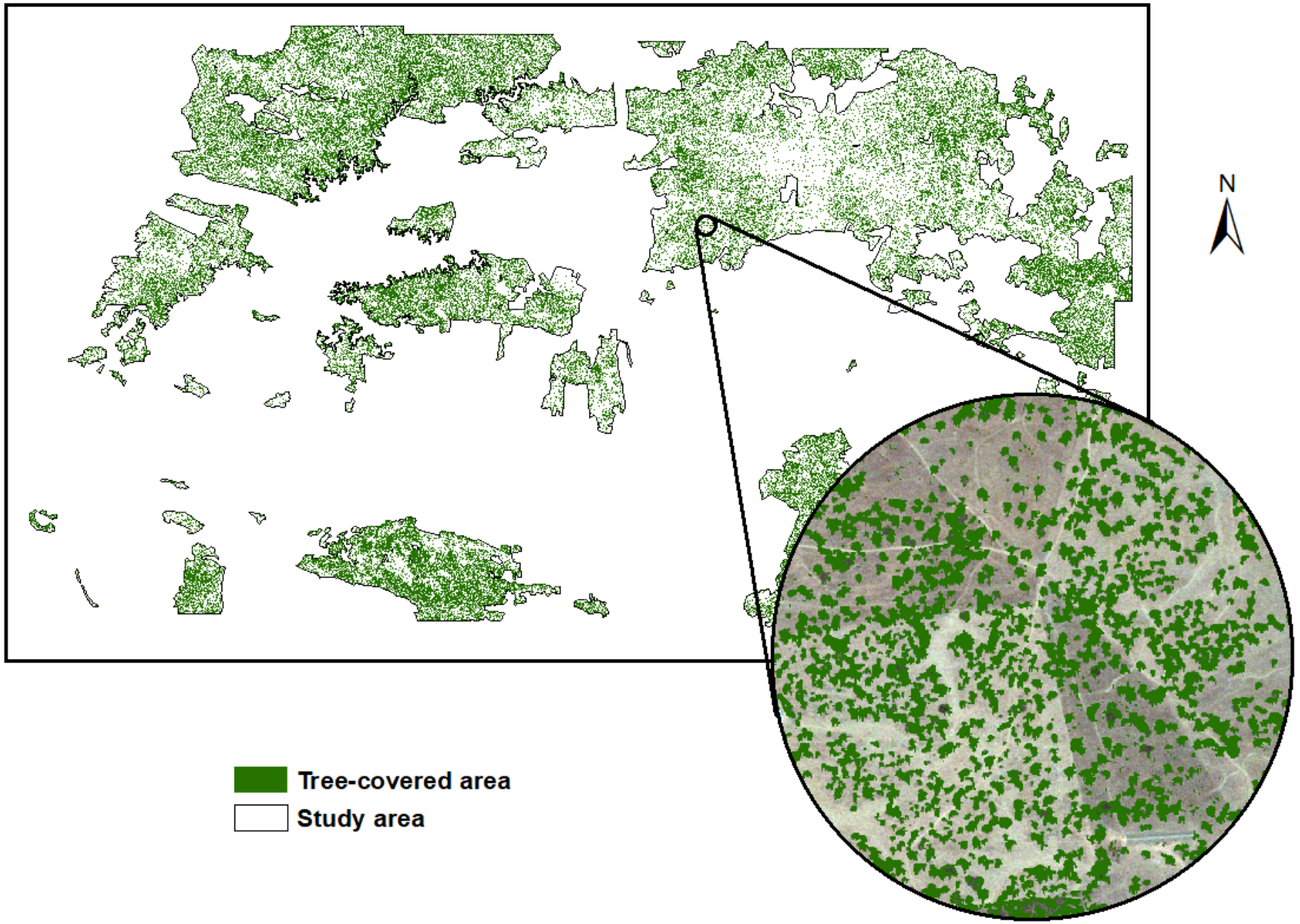

Table(Supplementary Material)
Click here to download Table: Table SM1.docx

Table SM.1.-Significance values (p) of ANOVA and/or Welch t-tests of model descriptors for affected/healthy trees each study date (Welch t-test was used when homocedasticity was not achievable even with the transformation of variables)

	ELV	SLOPE	TMI	WATER	ROADS	REFOR	RESEV	URBAN
2001	n.s. 0.3801	*** <2e-16	*** <2e-16	n.s. 0.641	*** 7.4e-14	*** <2e-16	* 0.018	ns 0.494
2009	n.s. 0.3831	*** 1.4e-12	*** 1.939e-6 (Welch)	*** 0.000124	*** <2e-16	*** <2e-16	*** <2e-16	*** <2e-16
2016	** 0.001766 (Welch)	*** <2e-16 (Welch)	n.s. 0.2815 (Welch)	*** <2e-16 (Welch)	n.s. 0.233	** 0.00323	*** <2e-16	*** <2e-16 (Welch)

Signif. codes: 0 '***' 0.001 '**' 0.01 '*' 0.05 '.' 0.1 ' '